Effect of nanoparticle additives on the tribological behavior of oil under boundary lubrication

by

Yosef Jazaa

A dissertation submitted to the graduate faculty

in partial fulfillment of the requirements for the degree of

DOCTOR OF PHILOSOPHY

Major: Mechanical Engineering

Program of Study Committee:
Sriram Sundararajan, Major Professor
Pranav Shrotriya
Sonal Padalkar
Scott Chumbley
Wenyu Huang

The student author, whose presentation of the scholarship herein was approved by the program of study committee, is solely responsible for the content of this dissertation. The Graduate College will ensure this dissertation is globally accessible and will not permit alterations after a degree is conferred.

Iowa State University

Ames, Iowa

2018

TABLE OF CONTENTS

Page

LIST OF FIGURES

Page

LIST OF TABLES

Page

ACKNOWLEDGMENTS

I would like to express my special appreciation and thanks to my advisor Professor Sriram Sundararajan, who has been a tremendous mentor for me. I would like to thank him for encouraging my research and for allowing me to grow as a research scientist. His Your advice on both research and my career have been priceless. I would also like to thank my committee members, professor Pranav Shrotriya, professor Sonal Padalkar, professor Wenyu Huang, and professor Scott Chumbley for serving and for all their brilliant comments and suggestions.

The thesis dissertation marks the end of a long and eventful journey for which there are many people that I would like to acknowledge for their support along the way. I would like to extend my appreciation to all members of Multiscale Surface Engineering and Tribology Laboratory, and Warren Straszheim from Material Characterization Research Laboratory for his collaboration in material characterization.

I would also like to extend a special thank you to my family. Words cannot express how grateful I am to my mother and father for all of the sacrifices that they have made on my behalf. Their faith in me was what sustained me thus far, without which I would have struggled to find the inspiration and motivation needed to complete this dissertation. I would like express appreciation to my beloved wife, Eman, who spent

sleepless nights with me and was always my support in the moments when there was no one to answer my queries.

Finally, I would like to thank John Deere and Iowa State University for partially funding this study. I would also like to acknowledge scholarship support provided by Jazan University, Saudi Arabia.

ABSTRACT

In this study, three different nanoparticles (CuO, WC, WS_2) of comparable nominal diameter, were added to a Polyalphaolefin (PAO) base oil to evaluate tribological response in the boundary lubrication regime. The concentration of particles was fixed at 1% by weight for this study and different surfactants (Oleic acid, polyisobutylene succinimide) and dispersion methods were employed to determine the impact on agglomeration and the observed tribological response. The results showed that of the methods studied, adding 10 % Oleic acid (OA) while sonicating the particles for 30 minutes reduced the agglomeration the most and adding 1% Oleic acid while sonicating the particles for 120 minutes produced a more uniform dispersion. Furthermore, this study investigates the effect of the surface treatment of MoS_2 and WS_2 on their tribological behavior in boundary lubricant regime The nanoparticles were dispersed in Polyalphaolefin (PAO) using the following techniques: 1) 60 minutes sonication without using a stabilizing agent, 2) 60 minutes sonication with 1% of weight Oleic acid (OA), and 3) functionalizing the nanoparticles using polyvinylpyrrolidone. The size distribution of the dispersed nanoparticles in PAO was measured by dynamic light scattering. The nanoparticles functionalized using Polyvinylpyrrolidone resulted in the most stable particles size and homogeneous mixture dispersion. Friction studies show that the introduction of nanoparticles additives does not appreciably impact the friction of the

interface for most cases in comparison to the base oil. Reciprocating wear experiments showed that the addition of nanoparticles without surfactants did not significantly increase the wear resistance compared to the base oil. Finally, this study investigates the dispersion techniques for CuO and WC nanoadditives on their effect on the rolling contact fatigue, using the best oil formulation that provided a stable suspension and agglomeration reduction for both materials. Tungsten carbide nanofluids showed the best micropitting resistantance behavior followed by copper oxide nanofluids under the boundary lubrication regime. Agglomeration reduction and homogeneous particles dispersion contribute to the wear reduction. The results of the friction and wear studies contributes to a better understanding of the tribological mechanism of the nanoadditives in base oil and clarify the difference between reducing agglomeration and improving dispersion. In this study, it is hypothesized that the additives might deposit on the surface and forming a physical tribofilm. In addition, if the nanoparticles fill the gaps between the surface roughness asperities which increase the true contact area, the particles can assist in movement like a nanoscale ball bearing. Depending upon the nanoparticles used, of evidence both mechanisms were found.

CHAPTER 1. INTRODUCTION:

1.1 Background and Motivation

The word tribology is derived from the Greek word *tribos*, which means the study of things that rub or simply rubbing [1]. Tribology, as a field, aims to understand and improve the reliability, efficiency, and overall performance of contact surfaces in motion [1]. Tribology encompasses fields including friction, wear, and lubrication [1]. The importance of improved understanding of the behavior of contact surfaces in relative motion is critical and has a wide-ranging impact on science, technology, and the economy. This effect is better summarized by the losses resulting from the lack of tribology considerations in the United States, which amount to a yearly $100 billion [2]. It has been estimated that developed countries can save up to 1.6% of the gross national product (GNP) [2], in the United States that would amount to approximately $300 billion (2016) [3]. A paper written by Kenneth H. (2016) stated that tribological contacts contribute about 23% of the World's total energy consumption, a staggering 20% to overcome friction, and 3% to remanufacture worn and spare parts due to wear-related failures [4].

tribologists consider modern tribology started when Leonardo da Vinci theorized the laws governing the motion of a rectangular block sliding over a planar surface about 500 years ago. Later, in 1699, Guillaume Amontons published the first formal account of the classical, macroscopic friction laws. He observed that the friction force is independent of the area of the surfaces in contact and the friction force is proportional to the applied load. Frictional force is defined as the force needed to move a certain surface divided by the weight of the load. Friction is usually represented by the friction coefficient (COF). Consider two blocks on top of each other, at the movement the entire weight if the top block is carried

by the high points in contact with each other as shown in Figure 1.1. The weight of the upper block is trying to crush the asperities peaks or move.

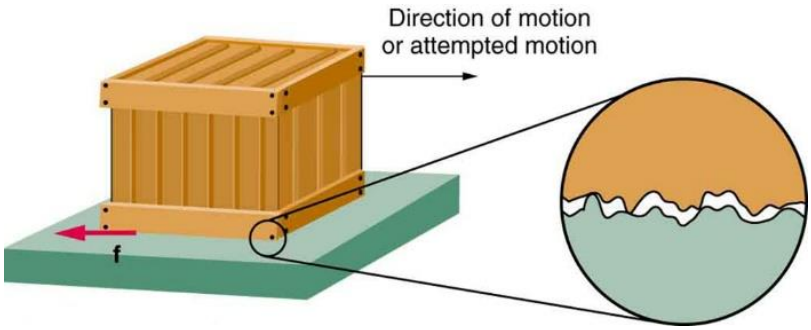

Figure 1.1 Friction is caused by interactions at the surfaces of adjoining parts [5].

At the nanometer scale, the surface area to volume ratio for a typical component is very high, surface forces become the dominant forces governing the contact behavior. At nanoscale level all surfaces are rough even at highly polished surfaces the load on the surface is supported by the surface asperities. Therefore, the friction between two contacted components has many sources such as microscopic welding, surface roughness hills and valleys mesh together, and the natural fraction force of two surfaces rubbing against each other. In dry contact the surfaces need to great amount of force to overcome the effects of friction.

Wear is the loss of material from due to contacting surfaces resulting from mechanical action in relative motion. Wear can affect national productivity, quality of life, and personal safety. Surface properties like hardness and elasticity of the material can affect the wear mechanism. Contact between surfaces is limited to a small portion of the apparent area. Therefore, contact stress between asperities must be in consideration when conducting a tribology experiment. Surface properties like hardness and elasticity of the material can affect the wear mechanism. The surfaces asperities subjected to greater deformation results in

increased number of contacts. Surface topography also can affect the wear and friction outcome, surfaces have different characterization forms such as waviness and roughness parameters.

Figure 1.2 shows three important wear mechanisms. Abrasive wear arises whenever hard, rough surfaces are ground against other surfaces of equal or less hardness. There are two main types of abrasive wear, two body and three body wear abrasive wear. Abrasive characterized by Unidirectional scratchers (severe) and polished surfaces (mild). The amount of wear depends on temperature, speed, surface finish, material, lubricant, and viscosity.

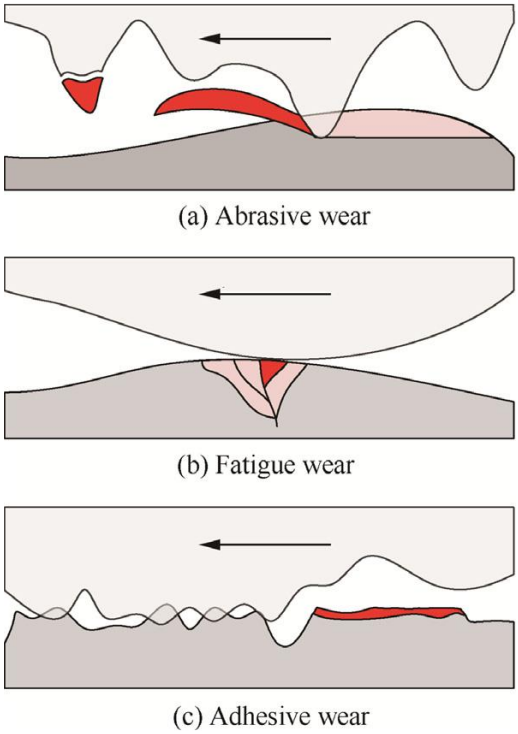

Figure 1.2 Abrasive, surface fatigue, and Adhesive wear mechanisms [6].

Another dominate wear mechanism is surface fatigue. Surface fatigue is caused by oscillating stress results in crack formation and surface deformation. Two basic types of surface fatigue are contact fatigue and micropitting. Interaction of the contact asperities, while subsurface fatigue cracks are due to high shear stresses, arise from residing inclusions

near the maximum Hertzian contact stress. The Hertzian contact stress usually refers to the stress close to the area of contact between two spheres of different radii. Hertzian subsurface shear stress is maximal just below the surface-subsurface cracks propagate parallel to the contact surfaces. Moreover, inclusions act as stress raisers leading to localized plastic deformation and crack nucleation, which will depend on the stress level and the number of cycles [5]. In rolling contact, it is recommended to improve the lubricant and reduce friction as much as possible because the contact loses efficiency due to friction. In 1999, Nelias *et al*. published a paper where they concluded that a surface initiated fatigue crack is due to local friction. Likewise, micropitting is caused by combined rolling and sliding action. Maximum shear stress occurs at the surface enhanced by high load, high friction, and rough surfaces. Micropitting is typically found in gear teeth dedendum, where surfaces experience opposing rolling and shear stress. Adhesive wear is also a dominate wear mechanism, strong adhesive forces between surfaces atoms cause materials to bind bound on contact. Under heavy sliding load, the surface asperities slide past each other and with the high temperature the asperities may weld and hold them until the surface tears and may result in adhesion wear.

The third critical aspect of tribology is lubrication, where primary function is to reduce friction and wear between interaction surfaces by reducing the load on the contact surfaces. The goal of adding lubricant is to improve the component lifetime by improving durability and reliability and lower the possibility of failure. For many years, various liquid oils and greases have been used as lubricants to make one surface slide smoothly over another, such as bearings or pistons in their chambers or wheels on their axes.

Industrial components operate under a variety of lubrication conditions: hydrodynamic, mixed, and boundary, with mixed and boundary being the predominant

regimes. Changes in the frictional properties are represented through what is known as *Stribeck* curves (Figure 1.3). The German scientist and engineer, Richard Stribeck, investigated the film-forming properties of lubricants in journal bearings. Stribeck outlined very distinct correlation between frictional properties and films of lubricant formed between two surfaces. The ratio of the fluid film thickness to the composite surface roughness is known as the Lambda ratio [6]. Also, based on the Lambda ratio, lubrication conditions can be devised to different regimes: boundary lubrication, $\lambda < 1$. mixed lubrication, $1 < \lambda < 3$. and hydrodynamic lubrication, $3 < \lambda < 10$ (Figure 1.3).

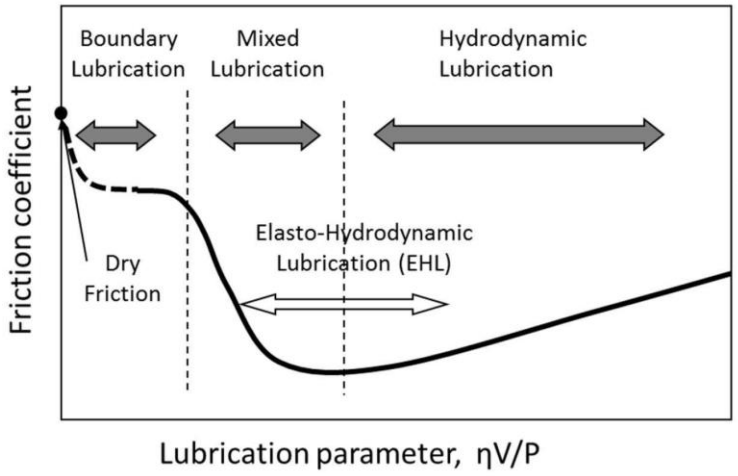

Figure 1.3 Schematic of the Stribeck curve; the friction coefficient as a function of the lubrication parameter: ηV/P. Where η is the fluid viscosity, V is the relative speed of the surfaces, and P is the load on the interface per unit width. [7]

At the hydrodynamic lubrication regime there is a relatively thick film of fluid between the moving surfaces, so no contact occurs between surfaces. The load in a hydrodynamic regime is carried out by the thick film of lubricant which separates the surfaces [1]. A mixed lubrication regime deals with the condition when the contact speed is low, the load is high, or the viscosity reduced. It occurs between the regions of no metal to metal contact and when there is a contact and some load is carried out by the surfaces

asperities. Boundary lubrication happens during sliding or rolling motion with metal to metal contact occurred between two surfaces. When the load is high, and/or the speed is low, the contact occurs at the peaks and hills of the surfaces asperities. In a boundary lubrication regime the normal load is supported by the asperities and the thin fluid film. At the point contact the surface has the most damage because of the high load at that point. Hence, boundary lubrication is a critical regime and typically governs the life of the components subjected to wear.

Studies have shown that tribological behavior of a lubricant can be improved by dispersing a small amount of nanomaterials base oil. [8]–[14]. Adding nanoparticles to oil can also be defined as nanofluid. In general, studies showed that adding nanoparticles enhanced some properties like viscosity, friction and wear reduction, and heat transfer. There are various dissimilarities in reported papers of nanofluids about their best performance improvement. For example, the studies summarized in Table 1 contain many variables.

Table 1.1 Summary of different nanofluid studies.

Lubricant	**Nanomaterial**	**Parameters studied**	**Findings**	**Reference**
Polyalphaolephin (PAO)	MoS2 nanotubes	friction and wear behavior	The coefficient of friction was decreased by more than 2 times. Wear loss reduced 5-9 times	[15]
CD15W-40 base oil	serpentine, La(OH)3 and serpentine/La(OH)3	friction-reducing and anti-wear properties	the lubricating oil containing serpentine/La(OH)3 composite particles exhibited better tribological	[16]
SAE40 engine oil	Copper and titanium oxide nanoparticles and single-walled carbon nanohorns (SWCNHs).	Different kinds of nanoparticles were tested as additives to engine oil to improve lubrication.	Friction was reduced, compared to raw oil	[12]

Table 1.1 continued

PAO	Oleic acid-capped core-shell lanthanum borate-SiO2 composites	The friction and wear behaviors	Containing OCLS possesses much better tribological properties than that of pure PAO and PAO containing SiO2 additive	[17]
Polyalphaolefin (PAO)	nanocarbon additives	Coefficient of friction (COF) and wear	Effect on the COF was accompanied by a reduction in wear with the addition of carbon nanotubes and NGP	[18]

Hence, the preparation techniques of nanofluid are the primary factor in their influence. Therefore, studying the impact of additives is not trivial because size, shape, concentration, and the particle materials are all critical factors that influence the lubrication performance [9][10]. Nanoadditives do not always improve tribological properties. Some nanoparticles which are hard and under heavy pressure or high particle concentrations in the area of contact can have an abrasive affect and increase friction and wear [19]. Increases in friction and wear were observed due to the agglomeration behaviors of nanoadditives[20].

The largest obstacle in preparing nanofluid is to find a formulation that provides higher stability and higher tribological performance. Due to high surface energy nanoparticles tend to agglomerate when added to oil. Typical powder particles stick together by weak or strong forces. According to DLVO theory (named after Boris Derjaguin, Lev Landau, Evert Verwey and Theodor Overbeek), there are two forces between nanoparticles, one is an attractive force between nanoparticles known as is Van der Waals, while the other is electrical double layer repulsive force [21]. When particles agglomerate, they stick together in a loosely coherent form. Furthermore, dispersing nanoparticles in the lubricant is still a challenging process as it tends to agglomerate as a result of the strong Van der Waal forces [5], [22]–[24]. Also, dispersing techniques that could be beneficial to specific

nanomaterials might not be suitable or beneficial for other nanomaterials due to the varying surface energy, which further affects the efficacy [24], [25].

1.2 Research Objectives

The objective is to improve lubricants and study the tribological effects of nanomaterial additives on friction and wear under boundary lubrication (low lambda) conditions, to enhance the performance of the lubricant and increase the lifetime of the mechanical contacts. The study aims to enhance the current understanding of the tribological mechanism of the nanoadditives in base oil and clarify the difference between reducing agglomeration and dispersing improvement. This study is comprised consists of three main parts: (I) influence of surfactants on the tribological behavior of nanoparticle additives under boundary lubrication conditions, (II) surface treatment of WS_2 and MoS_2 nano additives effect on the tribological behavior in boundary lubricant regime, and (III) effect of nanoparticle additives on rolling contact fatigue.

Specifically, part (I) focuses on the use of use of different surfactants and dispersion methods to determine their impact on agglomeration and the observed tribological response in the boundary lubrication regime. Three different nanoparticles with different relative hardness (CuO, WS_2, WC) were added to Polyalphaolefin base oil at 1% by weight, based on findings from previous studies [10], [26], [27]. These particles had a comparable nominal diameter and spherical shape.

Part (II) presents further investigation of WS_2 and MoS_2 nanoparticle additives in base oil to improve their dispersion and tribological behavior in boundary lubricant regime, with focus on the impact of surface tratments in order to reduce agglomeration and achieve a stable dispersion. The outcomes alleviate the understanding of the tribology behavior mechanism of WS_2 and MoS_2 nano additives in a boundary lubricant regime. This

investigation helps to discover if there is a correlation between the WS_2 and MoS_2 nano additives stability on the coefficient of friction and wear scar depth reductions in a boundary lubrication regime.

In part (III) nanoparticles with spherical shape and different relative hardness (CuO, and WC) were added to base oil by the best dispersion technique determined from the previous experiments to enhance the performance of the lubricant to increase the lifetime of the mechanical contacts. Testing of the agglomeration reduction and the difference in materials hardness will show dissimilar behavior in reducing shearing force and minimize microprinting on the surface.

1.3 Dissertation organization

The rest of this Dissertation is divided into four chapters. Chapter 2, focuses on the aspects of part (I), and the use of different surfactants and dispersion methods to determine their impact on agglomeration and the observed tribological response in the boundary lubrication regime. Chapter 3 focuses on the aspects of part (II), and presents further investigation of WS_2 and MoS_2 nanoparticle additives in base oil to improve tribological behavior in a boundary lubricant regime. Chapter 4, focuses on the aspects of part (III), in which different nanoparticles with spherical shape and different relative hardness (CuO, and WC) were added to base oil by the best dispersion technique determined from the previous experiments to enhance the performance of the lubricant to increase the lifetime of the mechanical contacts. In Chapter 5, conclusions from different chapters are summarized. Experimental instruments and methods used related to each study are mentioned in the respective chapters.

CHAPTER 2. INFLUENCE OF SURFACTANTS ON THE TRIBOLOGICAL BEHAVIOR OF NANOPARTICLE ADDITIVES UNDER BOUNDARY LUBRICATION CONDITIONS

Y. Jazaa and S. Sundararajan "Influence of surfactants on the tribological behavior of nanoparticle additives under boundary lubrication conditions" submitted to Tribology International.

2.1 Abstract

1% by weight of CuO,WC, and WS_2 nanoparticles were added to a Polyalphaolefin base oil to evaluate tribological response. Different surfactants were employed to reduce agglomeration. The results showed that adding 10 % Oleic acid (OA) while sonicating the particles for 30 minutes reduced the agglomeration the most, and adding 1% OA while sonicating for 120 minutes produced a more uniform dispersion. Friction studies showed that the nanoparticles additives do not appreciably impact the friction compared to base oil. Wear resistance was improved by about 60% for CuO and WC with 1% OA and sonicated for 120 minutes. The study suggests that conditions that minimize agglomeration and promote high dispersion lead to favorable wear resistance under boundary lubricant conditions.

2.2 Introduction

Research has shown that adding nanoparticles to the lubricants can improve the tribological behavior of the lubricant [9]–[13], [28]. Studying the impact of nanoparticle additives is not trivial because size, shape, concentration and the particle materials are all critical factors that influence the lubrication performance. A range of metallic nanoparticles and related oxides and disulfides have been investigated. These studies showed that adding nanoparticles reduced both friction and wear, with improvements for specific materials of up to two-five times compared to the lubricant without nanoparticles [12], [29].

The literature suggests that lower sized nanoparticles, ranging from 30 nm to 300 nm in

diameter, reduce friction and wear most on contact surfaces [8], [30], [31]. The shape of the nanoparticles was not investigated in these studies, but it is commonly believed that spherically shaped particles are favorable for rolling in the contact area and reducing friction [10]. Other studies investigated the impact of different concentration of the additives in the lubricant. Overall, 1% of nanoparticles by weight was recommended to be used for a variety of materials [10], [32]–[34].

Studies have shown that agglomeration of nanoparticles occurs when they are dispersed in oil as additives in oil [13], [35]–[39]. The use of surfactants has been reported to alleviate this problem [40]–[43]. A majority of the studies have shown improvements in particle stability by bath-sonicating the suspension, adding a surfactant to the particles, or using a combination of both techniques in order to alleviate agglomeration and improve the wear and friction reduction of the lubricant [5], [36], [37], [44]–[46]. The agglomeration of the dispersed particles can be reduced by intensive ultrasonication and adding a suitable amount of surfactant, and the choice of nanoparticle dictates the specifics of the dispersion methods[25]. A suitable surfactant can decrease the attractive force between nanoparticles, thus reducing surface energy and tendency to agglomerate [24]. However, most of these studies do not report the extent to which agglomeration exist in their samples.

Regarding the lubrication regime, a large number studies have investigated the influence of nanoparticle additives in the mixed lubrication regime [5], [9], [47]–[53]. Relatively fewer studies have been carried out under boundary lubrication regime [15], [54]–[56] . While these studies suggested that nanoparticle additives were not significantly effective in boundary lubrication as compared to the mixed lubricant regime [57]–[59], they did not address the impact of any agglomeration that may have occurred.

In this study, three different nanoparticles with different relative hardness (CuO, WS_2, WC) were added to base oil at 1% by weight, based on findings from previous studies [10], [26], [27]. These particles had a comparable nominal diameter and spherical shape. This study focused on the use of different surfactants and dispersion methods to determine their impact on agglomeration and the observed tribological response in the boundary lubrication regime.

2.2 Experimental:

2.2.1 Materials:

Table 2.1 Selected physical properties of the nanoparticles used in the study.

Nanoparticles	**Density[a] (g/m^3)**	**Hardness[b] (mhos)**	**Surface Energy[c] (mJ/m^2)**
CuO	6.4	3.5	0.76
WC	15.63	9	1.19
WS_2	7.5	0.75	15.499

a: Manufacture specification.
b: Obtained from references [60]–[62].
c: Obtained from references [63]–[65].

The base oil used in this study was Polyalphaolefin (PAO) provided by Exxon mobile corporation. The manufacturer specifications for the oil were: relative density 0.85 at 15°C, and viscosity 400 cSt at 40°C. The lubricant did not have any additives. CuO, WC, and WS_2 were selected as nanoparticle additives (purchased from Zhengzhou Dongyao Nano Materials Co., Ltd., China). Selected properties of the nanoparticles, as reported by the manufacturer are listed in Table 2.1. In order to better isolate the effect of the materials, the nominal size (100 nm) and shape (spherical) of the particles were selected to be comparable. However, as shown in Figure 2.1, TEM images of the nanoparticles (ethyl alcohol was used as a solvent

for imaging) indicate that a size distribution exists, and agglomeration further impacts any notion of nominal particle size.

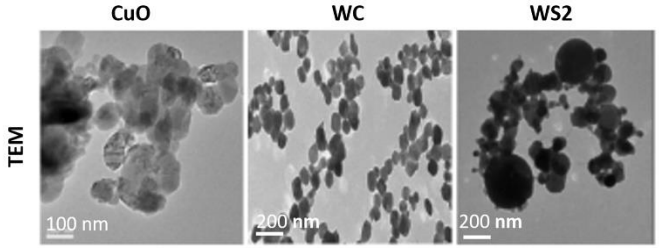

Figure 2.1 TEM images of the nanoparticles used in this study.

In this study, two surfactants were used, Oleic acid (OA) (Sigma-Aldrich), and polyisobutylene succinimide or PIBS (Soltex Inc) were used as surfactants. Oleic acid (OA) has been commonly used as dispersion agent to stabilize several nanomaterials in fluid [39], [41]–[43], [66], [67].

Likewise, Polyisobutylene succinimides (PIBS) have been used as detergent–dispersants in lubricating oils and previous studies have confirmed that PIBS helped to reduce the surface energy of the aggregated nano additives and improved dispersion [68]–[70]. The two surfactants are organic and have a polar functional group attached to long bulky hydrocarbon chains. These chains are nonpolar which enhance the solubility and dispersibility of nanomaterials in fluid by getting absorbed by the high surface energy of the nanoparticles.

In this study, the concentration of the nano additive in oil was chosen to be 1% by weight for each nanoparticle sample, based on recommendation from studies on a variety of materials additives [2,12–14,41,42.] Solutions were prepared with 1% of each nanoparticle by weight in 150 ml of base oil. In order to investigate the effect of surfactant on agglomeration, solutions with the nanoparticle to surfactant weight ratios of 1:1 and 1:10

were prepared, which represent the typical level and lower level of surfactants in prior studies [2], [11], [15], [23]. From initial studies, it was found the particles size did not vary for sonication times of 30 to 120 minutes. Consequently, all samples were prepared by treating the nanoparticles by mixing the appropriate amounts of surfactant and nanoparticles, to promote surface modification of the particles. This mixture was subsequently added to 150 ml of oil and ultrasonicating in a water bath for 30 or 120 minutes prior to analysis or testing.

For this study, a spherical SiC probe (4 mm diameter, hardness = 9 mohs, v = 0.19, E = 415 GPa) and an AISI 8620 steel substrate (4.5 mohs hardness) were used. The average substrate surface roughness (Ra) was approximately 0.025 μm as measured by Zygo NewView 7100 non-contact profilometry over a scan area 0.47 mm × 0.35 mm using 20X objective.

2.2.2 Methods:

In order to obtain a better estimate of the nominal particle size in solution, the size distribution of dispersed nanoparticles in PAO was measured by dynamic light scattering (DLS) (Malvern ZetaSizer Nano ZS). The theory underlying the measurements of the Zetasizer are based on effects of Brownian motions of nanoparticles on Rayleigh light scattering [35][67]. Following sample preparation, DLS data were collected over a space of 1 hour for each sample. The data represents the hydrodynamic diameter distribution of the particles in solution. Three replicate tests were conducted for each sample formulation. Data was reported as an average of three measurements along with the 90% confidence interval.

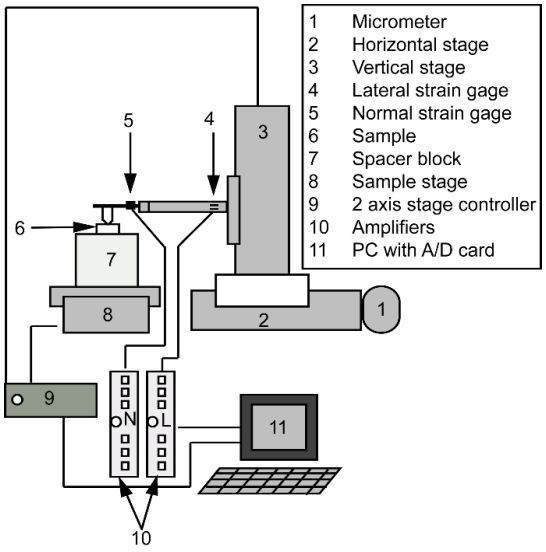

Figure 2.2 Schematic of Microtribometer used for friction and wear tests.

For the friction and wear experiments, a custom-built reciprocating ball-on-flat microtribometer that can produce a microscale (apparent area ~1000 μm^2) multi-asperity contact was used [71]. A schematic of the microtribometer major components is shown in Figure 2.2. A probe with a specific radius is placed at the end of a crossed I-beam structure which is lowered using a linear stage to apply a desired normal load to the sample.

The normal and the friction (lateral) forces in the microtribometer are measured using semiconductor strain gauges on the cantilevers. Friction forces can be resolved to approximately ±5 μN and normal forces to approximately ±15 μN. The signal from the normal load is monitored and used in a simple proportional-integral (PI) feedback loop to maintain the desired normal force regardless of any slope or waviness in the surface of the sample. The desired sample is affixed to another stage set perpendicular to the beam, which provides linear motion.

150 ml of each additive formulation was added to the substrate prior conducting test, a new steel substrate and a new SiC probe was used for each friction and wear test. To

evaluate the coefficient of friction the applied normal load was increased linearly from 0 to 2000 mN over a specific sliding distance of 25 mm at a speed of 1 mm/s. Based on these parameters, the maximum Hertzian contact pressure was estimated to be 1.2 GPa, and the lubrication regime was boundary lubrication. The lateral force was recorded to compare with the normal force generating a coefficient of friction represented as the slope of the data plot. Five replicates were conducted for each condition and the average values were reported along with the 90% confidence interval. In order to obtain wear response, reciprocating sliding wear test were performed against the SiC probe at a constant load of 2000 mN for 100 cycles, a stroke length of 8 mm and a stroke speed of 10 mm/s. Two replicates were conducted for each test condition per sample for each wear track, and reported along with 90% confidence interval. An average wear depth was reported from five measurements which averages the wear track using the Zygo profilometer, after cleaning the substrate with Isopropyl Alcohol. Note that base oil (with no additives) was used as a control.

An FEI Quanta-250 Scanning Electron Microscope (FESEM) was used to obtain high-resolution images of wear tracks, and Oxford Aztec energy-dispersive X-ray analysis was used to perform point analysis of the wear track and adjacent regions for evidence of any tribofilm formation. Backscattered images were analyzed for further tribofilm analysis with an accelerating voltage 10 kV and spot size 4 A.U. for all cases.

2.4 Results and discussions:

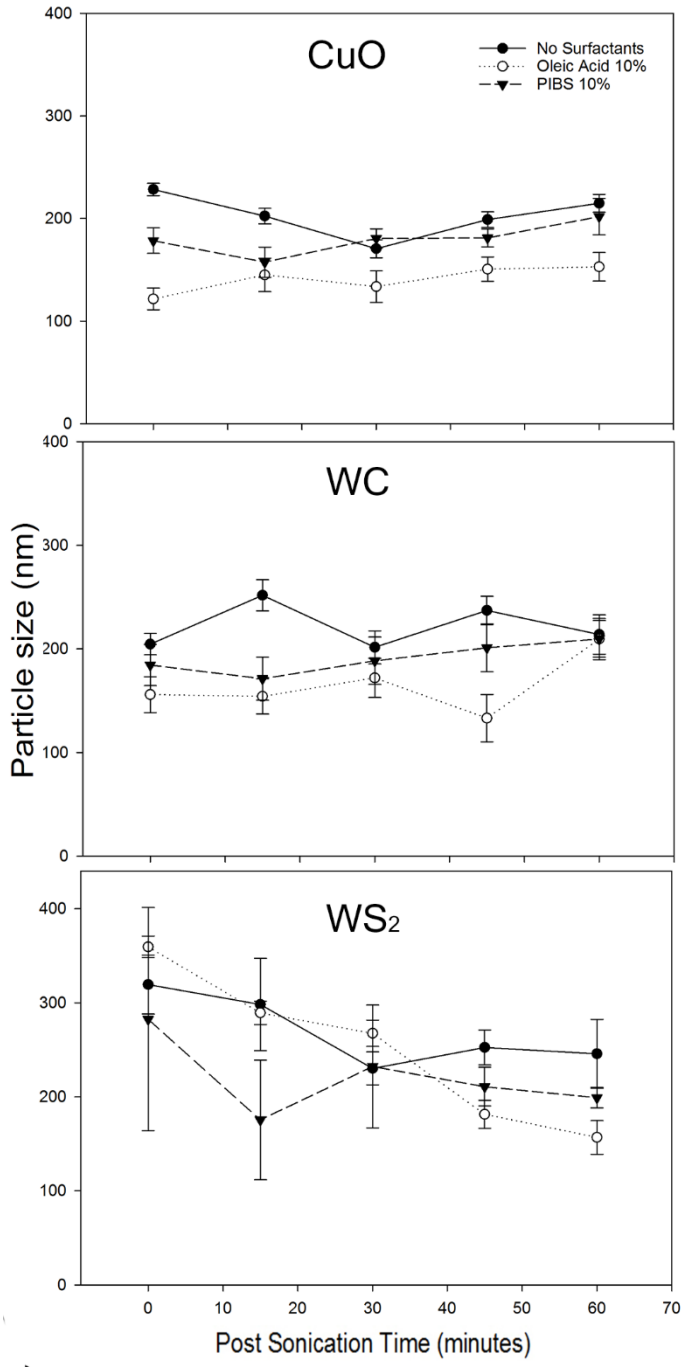

Figure 2.3 Dynamic light scattering (DLS) data showing average hydrodynamic diameter of nanoparticles in PAO as a function of post sonication time (30 minutes), with and without surfactants.

Figure 2.3 shows the average particle size in PAO as measured using DLS for the various combination of nanoparticles (1% by weight) and surfactants (10% by weight) as a function of post sonication time (30 minutes). The reported nominal particle size was 100 nm, but the DLS data shows that the average particles size in PAO range from about 200-250 nm for CuO and WC, 200-350 nm for WS_2. The data suggests that some agglomeration may be occurring for all particles, with WS_2 showing the largest propensity to agglomerate. The variance in agglomeration behavior is due to differences in physical properties and surface energy of the materials [25]. The addition of surfactants appears to reduce the observed average particle sizes to varying degrees. For CuO and WC, Oleic acid seems to be the most effective surfactant, resulting in average particles sizes of 150-180 nm or below, compared to 180-200 nm with PIBS. This suggests that Oleic acid helps to minimize the Van der Waals forces of attraction between particles for CuO and WC more than PIBS, leading to a minimal number of nanoparticle aggregates in the oil. On the other hand, WS_2 exhibited much higher variation in particle size despite the addition of surfactants presumably due to its high surface energy compared to the other particles. The addition of Oleic acid seems to gradually reduce the particle size up to 60 minutes post sonication time, resulting in an observed particle size of about 150-180 nm at 60 minutes, compared to 200 nm for PIBS. While the addition of a surfactant can form a layer on the nanoparticle surface and contribute to an increased diameter, the data suggest that agglomeration is the greater contributor to increased diameters. This is supported by the fact that the observed diameters for particles with surfactants lower to that of particles without surfactant. Based on these results, Oleic acid was chosen as the surfactant for the subsequent tests to explore the effect of varying surfactant concentration and sonication time on resulting particles sizes. In order to focus on

the impact of the nanoparticles, a lower level of (1%) OA was chosen with different sonication times to compare with 10% OA and 30 minutes sonication.

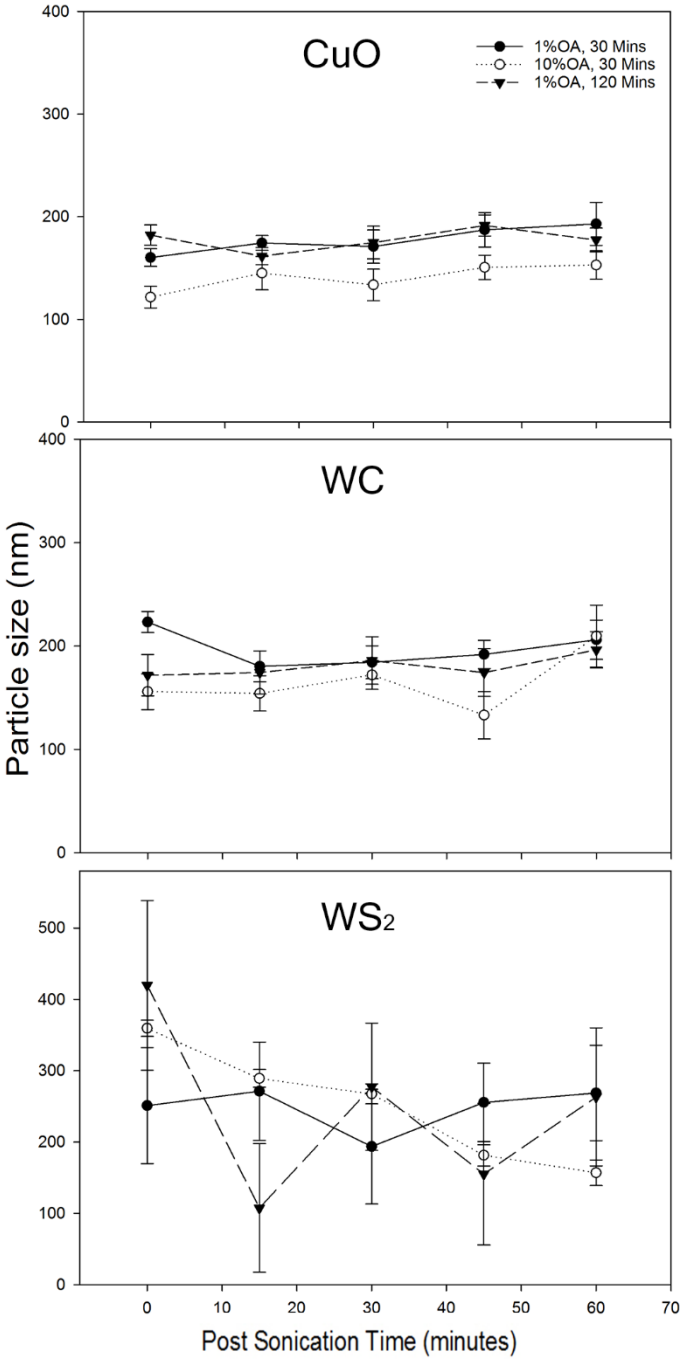

Figure 2.4 DLS data showing average hydrodynamic diameter of nanoparticles in PAO as a function of surfactant and sonication time.

Figure 2.4 shows the average particle size as measured using DLS for the nanoparticles additives (1%) in PAO with different amount of OA (1% and 10%) and sonication times (30 minutes and 120 minutes). CuO dispersed with 1% OA and sonicated for 30 minutes resulted in average particle size of 177 nm at 10 minutes post sonication, after which the particles size increases gradually to about 200 nm at 60 minutes post sonication time. When CuO was dispersed with 1% OA to in PAO and sonicated for 120 minutes; the average particle size reduced to about 120 nm at 10 minutes post sonication time and increased modestly to about 177 nm at 60 minutes post sonication time. CuO particles with 10% OA and sonicated for 30 minutes resulted in the lower average particles sizes of 150 nm or below, but the particles size fluctuated in a range ± 30 nm during the 60 minutes post sonication.

Dispersing WC particles in PAO with 1% OA and 30 minutes sonication resulted in a particles average of 200 nm, while the sonication for 120 minutes resulted in average particle size 175 nm. Adding 10% OA to WC particles and 30 minutes sonication, resulted in lower average particles size of 165 nm. In this case, particle size was settled for the first 30 minutes post sonication, after which it starts fluctuating within a range of ± 75 nm.

WS_2 particles continued to exhibit comparability highly variable particle sizes. Adding 10% OA, with 30 minutes sonication time resulted in a monotonically reducing trend for particle size up to 60 minutes after sonication, exhibiting a size of about 150 nm at the 60 minutes mark. Based on this data, tribological tests were conducted with nanoparticle additives dispersed in PAO with 1% OA and 120 minutes sonication and 10 % OA and 30 minutes sonication time, as these conditions appeared to result in lower observed particle sizes and/or stable values over time.

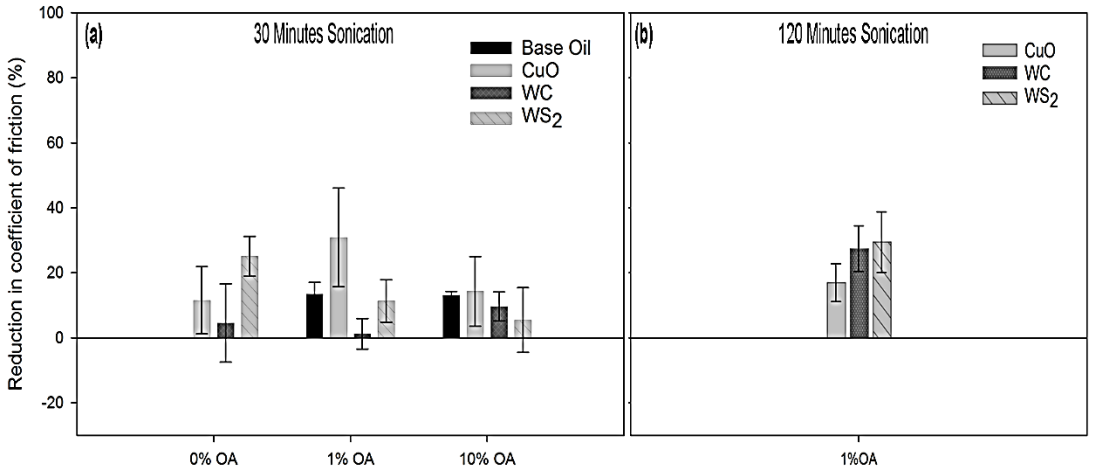

Figure 2.5 A comparison of the reduction in coefficient of friction exhibited by the various nanoparticle dispersions for (a) 30 minutes and (b) 120 minutes sonication time. Reductions are expressed as percentages with respect to the coefficient of friction observed in a base oil condition.

Figure 2.5 shows the relative reduction of the coefficient of friction for different nanoparticle dispersions, with various Oleic acid percentages as compared with the neat base oil (PAO). Figure 2.5 (a) shows data for samples sonicated for 30 minutes. The addition of nanoparticles without surfactant (0% OA) provided some reduction in COF, with WC showing high variability. We speculate that the high the variability in the case of WC with 0% OA was due the higher hardness of WC. The addition of OA to the base oil (PAO) provided additional lubricity (~10%), and is consistent with findings reported previously on the surface contact in boundary conditions [72]. The addition of OA (1% by weight) to improve the nanoparticles dispersion, surprisingly, did not result in statistically significant improvements to the friction response with CuO being the sole exception, but with high variability. Figure 2.5 (a) also shows that the addition of 10 % OA did not exhibit statistically valid differences in friction response for the for the particles and did not improve upon the behavior shown with 1% OA.

Figure 2.5 (b) shows the relative reduction of the coefficient of friction for the different nanoparticles dispersion when sonicated for 120 minutes with 1% OA compared with the base oil. This dispersion method resulted in a small additional reduction in friction for WC and WS_2 while CuO showed no improvement compared to the 30 minutes sonication condition. Our initial expectation was that conditions that minimized observed particle size (and hence agglomeration) might lead to better lubricity. However, the data suggests that agglomeration of the nanoparticles do not significantly impact lubricity under the specified testing conditions.

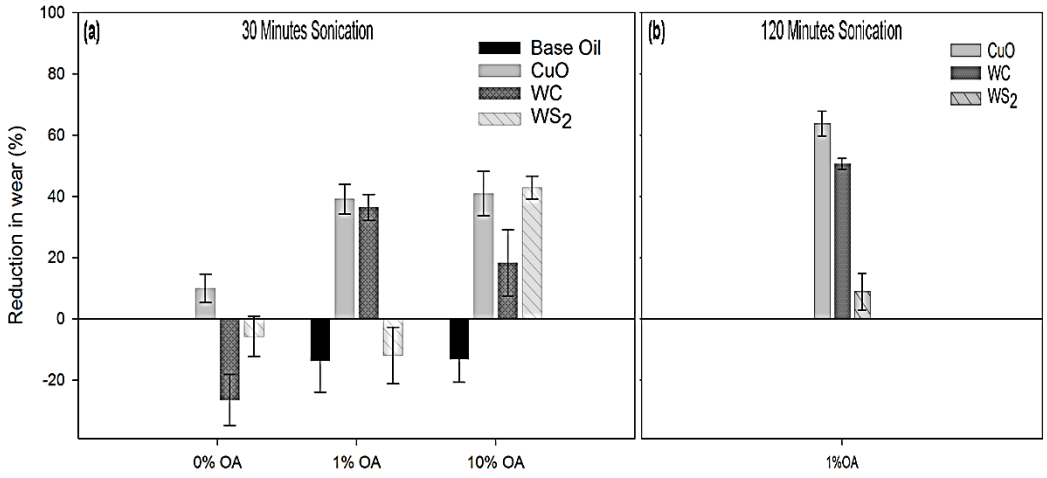

Figure 2.6 A comparison of the reduction in wear exhibited by the various nanoparticle dispersion for (a) 30 minutes (b) 120 minutes sonication times. Reductions are expressed as percentages with respect to the wear observed with just the base oil. Positive values indicate improved wear performance, whereas negative values indicate poorer performance.

Figure 2.6 (a) shows the average wear depth of different nanoparticles dispersed by sonication for 30 minutes and different Oleic acid percentages, compared with the neat base oil. The performance of the base oil with just Oleic acid added is also shown for comparison.

When nanoparticles were dispersed in base oil with no surfactant, only CuO exhibited an improved wear resistance (~10%). The addition of WC and WS_2 without OA decreased the wear resistance; it is possible this negative behavior is due to the presence of agglomeration of the nanoparticles. The higher hardness of WC can contribute to increased abrasive wear via third body interactions compared to WS_2.

The addition of OA (1% or 10%) to the base oil (without nanoparticles) actually led to poorer wear resistance. This is attributed to the increased surface deformation resulting from surface active organic acid that has been reported in literature [62,63]. Adding 1% OA to improve the nanoparticles dispersion resulted in an improvement of wear reduction by around 40 % for CuO and WC. WS_2 nanoparticles dispersed with 1%OA and 30 minutes sonication did not exhibit any improvements in wear resistance. This is attributed to the improvement in observed particle size for CuO and WC, but not for WS_2 with the addition of 1% OA (Figure 2.3).

Addition of 10% Oleic acid which resulted in lower or comparable observed particles size for CuO and WC, did not translate to improved wear resistance. In fact, WC with 10% OA showed poorer wear resistance compared to the 1% condition. WS_2, which exhibited lower particle size with 10% OA showed significant improvement in wear resistance.

Figure 2.6 (b) shows the average wear depth reduction percentage of the nanoparticles dispersed by adding 1% OA and sonicated for 120 minutes. CuO and WC showed their best wear resistance (63% reduction for CuO and 50% reduction for WC), compared to the wear depth with base oil. This was surprising since this dispersion condition did not show significant reduction in observed particle size compared to the condition. WS_2 exhibited poorer wear resistance compared to the 10% OA, 30 minutes sonication condition.

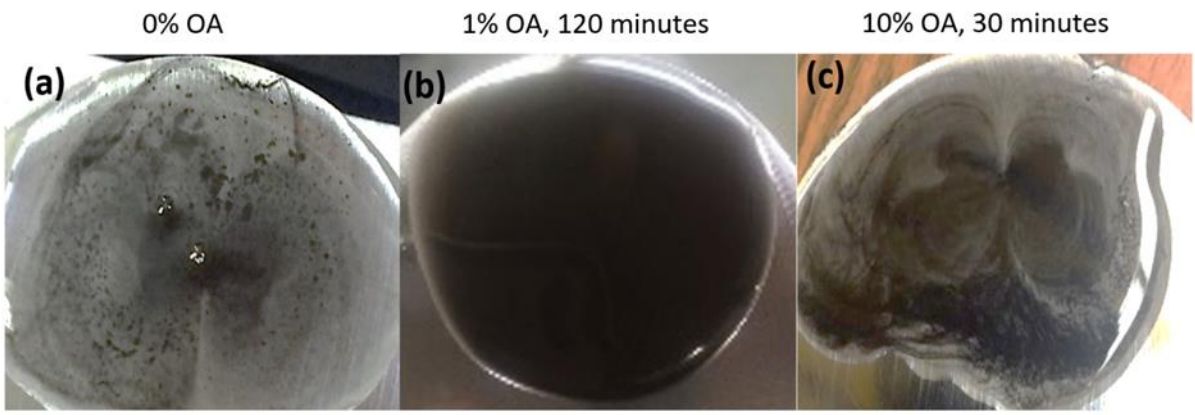

Figure 2.7 Optical images of CuO dispersed particles, showing differences in uniformity of dispersion for the various combinations of surfactants and sonication times.

Figure 2.7 shows optical images of the steel substrate surfaces covered by the lubricant with CuO additives after conducting wear test. For the conditions with 0% OA and 10 % OA and 30 minutes sonication time, the nanoparticles appear to exist in distinct regions, suggesting that they are not uniformly dispersed. On the other hand, the condition with 1% OA and 120 minutes sonication time shows no such segregation and appear to be more uniformly dispersed and homogeneous. This was the observation for WC as well. This helps explain why although the DLS data suggests slight differences between the two dispersion conditions, the condition of 1% OA with 120 minutes sonication produces better wear resistance for CuO and WC. There was no clear correlation between the observed WS_2 particle size and wear depth reduction because the particles size fluctuates significantly with time. However, the 10% OA formulation showed monotonically decreasing particle size and showed the best wear resistance. Thus the data suggest that conditions that minimize agglomeration and promote high dispersion lead to favorable wear resistance under boundary lubricant conditions, which is consistent with recommendations from other studies for other lubrication conditions [30]. This corresponds to using 1% OA and 120 minutes sonication for

CuO and WC and 10% OA and 30 minutes sonication for WS_2. It must be noted in the case of WS_2, 1% OA and 120 minute sonication time results in widely varying results (Fig.4) for observed size via DLS. Comparing CuO and WC the lower hardness of CuO promotes shearing of the particles compared to WC, thus contributing to higher friction and increased wear resistance.

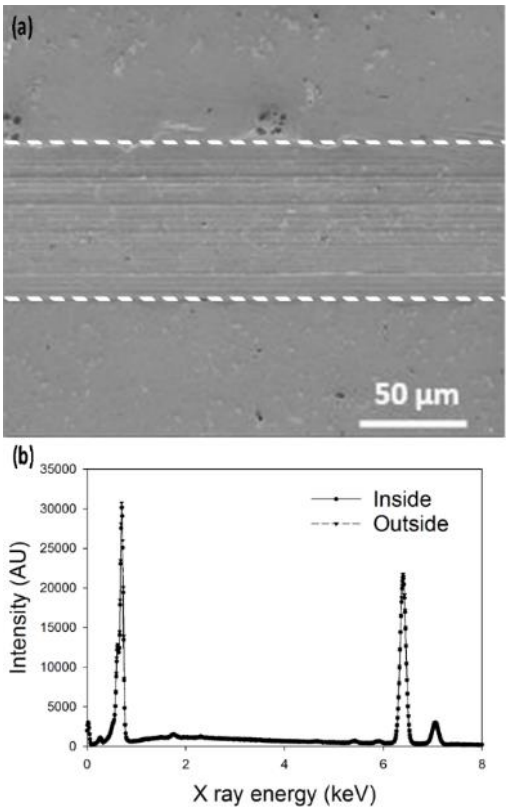

Figure 2.8 (a) Representative SEM image of a wear track on a steel substrate [CuO with 1% OA, 120 mins]. Dotted lines indicate the edges of the wear track. (b) EDS data from regions inside and outside the wear track, showing lack of any particles or particle-based film formation.

To help identify the prevailing wear mechanism for the lubricants with nanoparticle additives, the wear tracks were analyzed using SEM as shown representatively in Figure 2.8. Figure 2.8 (a) shows evidence of abrasive wear via ploughing for the sample tested using the lubricant with CuO particles (1% OA, 120 minutes sonification). In Figure 2.8 (b), areas

inside and outside the wear track were chemically analyzed using EDS to identify evidence of nanoparticle-based film formation. The data reveal no evidence of any nanoparticle-based material on any of the wear tracks. Analysis of SEM images and EDS data for the substrates tested using lubricant with WC and WS_2 nanoparticles yielded similar results. This suggests that for our testing conditions, the mechanism of wear reduction in the boundary lubrication condition is via load support of rolling nanoparticles rather than the formulation of a tribofilm. The agglomeration reduction and homogeneous particles dispersion help to make particles roll more, and contribute to the wear reduction. This is further evidenced by the fact that no nanoparticles adhered in the wear track, instead they remained free in the oil.

2.5 Conclusions:

The study investigated the tribological impact of adding different nanoparticles additives (CuO, WS_2, WC) to oil in boundary condition lubricant regime, including looking at factors that minimize nanoparticle agglomeration. The results showed that adding 10 % Oleic acid while sonicating the particles for 30 minutes reduced the particle size the most of the methods studied, and adding 1% Oleic acid while sonicating the particles for 120 minutes produced a more uniform dispersion. Friction experiments under boundary lubrication showed that adding nanoparticles can enhance lubricity to varying degrees (10 – 20 %) under different dispersion conditions. Minimizing agglomeration did not seem to be a necessary contribution for friction reduction.

Reciprocating wear experiments showed that the addition of nanoparticles without surfactants did not significantly increase the wear resistance compared to the base oil. CuO and WC additives exhibited increased wear resistance when tested with 1% of CuO and WC with 1% OA and subjected to sonication for 120 minutes. These conditions showed wear

depth reduction of about 63% for CuO and 50% for WC as compared to the wear depth observed for the base oil. WS_2 nanoparticles exhibited a 42% reduction in wear depth when tested with 10% OA and 30 minutes sonication. These dispersion conditions result in the best agglomeration reduction and dispersion for the corresponding particles. Chemical analysis and SEM observations of the wear surfaces showed that the particles promote wear resistance via load support as 'nanoball bearings' rather than via a tribofilm formulation.

Agglomeration reduction and homogeneous particles dispersion contribute to the wear reduction by increasing the true contact area and reducing shear forces on the roughness asperities. We believe that the nanoparticles additives provide better wear reduction results in cases when agglomeration has been minimized, and the particles are well dispersed.

Acknowledgments:

Partial funding for this work was provided by John Deere Product Engineering Center in Waterloo, Iowa and Iowa State University. The authors would like to thank Derek White for his assistance in wear depth analysis. Yosef Jazaa acknowledges scholarship support provided by Jazan University, Saudi Arabia.

CHAPTER 3. THE EFFECT OF AGGLOMERATION REDUCTION ON THE TRIBOLOGICAL BEHAVIOR OF WS_2 AND MOS_2 NANOPARTICLE ADDITIVES IN BOUNDARY LUBRICATION REGIME

Yosef Jazaa, Tian Lan, Sonal Padalkar and Sriram Sundararajan
Department of Mechanical Engineering, Iowa State University, Ames IA 50011, USA
Manuscript in preparation for submission to "Lubricants"

3.1 Abstract

This study investigates the impact of different surfactants and dispersion techniques on the friction and wear behavior of WS_2 and MoS_2 nanoparticles additives in a Polyalphaolefin (PAO) base oil under boundary lubrication conditions. The nanoparticles were dispersed in using Oleic acid (OA) and Polyvinylpyrrolidone (PVP) as surfactants to investigate their impact on particle agglomeration. The size distribution of the dispersed nanoparticles in PAO was measured by dynamic light scattering. The nanoparticles functionalized using PVP resulted in the most stable particles size and homogeneous mixture dispersion. Friction studies showed that nanoparticle agglomeration reduction and the homogeneity of the suspension do not significantly impact the friction reduction behavior of the lubricant. Reciprocating wear experiments showed that for our test conditions, both WS_2 and MoS_2 nano additives showed maximum wear depth reduction (45%) when using the PVP surface treatment compared to base oil. The wear results confirmed the significance of minimizing agglomeration and promoting high dispersion, leading to favorable wear resistance under boundary lubricant conditions. Analysis of the wear surfaces showed that a tribofilm formation was the primary wear reduction mechanism for WS_2 particles treated by PVP whereas in the case of MoS_2 treated by PVP, the mechanism was load sharing via particles rolling and/or sliding at the interface.

3.2 Introduction

Several studies have shown that tribological behavior of a lubricant can be improved by dispersing small amount of nanomaterials in base oil. Dispersing nanoparticles in lubricant is a challenging process as the particles tend to agglomerate due to strong Van der Waal forces [5], [23], [24]. The literature shows that dispersion of nanoparticles additives can be improved by using a number of techniques including sonicating, which includes both bath or probe sonication, adding a surfactant, or a combination of the aforementioned techniques [24], [35], [36], [40], [42], [44]–[46], [73]. Specifics of the dispersion method is dictated by the nanoparticles and their surface energy [24], [25].

In this study, we selected two dichalcogenides nanoparticles, WS_2 and MoS_2 that have been shown to improve tribological behavior as additives. The use of MoS_2 nanoparticles has been extensively investigated over the last few years. Several studies on MoS_2 nanoparticles did not use a surfactant to stabilize the nanoparticles when added to the lubricant [15], [74]–[78]. However, MoS_2 nanoparticles have a strong tendency to agglomerate when added to lubricants [78]–[80]. Other studies investigated the dispersion of the MoS_2 nanoparticles and showed that the agglomeration could be reduced by adding surfactant and via bath sonication [81]–[84]. Similarly there are studies that have demonstrated improved tribological behavior using WS_2 nanoparticle additives with [26], [57], [76], [85]–[89] and without [82], [84], [90]–[93] the use of surfactants. Nevertheless, these results suggest there is a need to determine if reduced agglomeration and dispersion stability directly contribute to improving tribological performance.

The present paper investigates the impact of different surfactants and dispersion techniques on the friction and wear behavior of WS_2 and MoS_2 nanoparticles additives in a

Polyalphaolefin (PAO) base oil under boundary lubrication conditions. Oleic acid (OA) and Polyvinylpyrrolidone (PVP) were chosen as surfactants. Both these materials are commonly used in the literature to stabilize nanomaterials additives,[44], [49], [94]–[97]. Our previous work [98] showed that while OA was effective in reducing agglomeration for CuO and WC nanoparticle additives, they were less effective for WS_2 particles. PVP has been shown to be effective for dichalcogenides due to reducing repulsive forces between its hydrophobic chains [82], [84], [99], [100].

3.3. Experimental:

3.3.1 Materials:

The neat base oil used in this experiment was Polyalphaolefin (PAO), with the following specifications as reported by the manufacturer (Exxon mobile Corporation): density 826 g/m^3 at 15°C, and viscosity 400 cSt at 40°C. WS_2 nanoparticles were purchased commercially (Zhengzhou Dongyao Nano Materials Co., Ltd., China) and had the following properties: a spherical shape with a nominal diameter of 100 (nm), density of 7.5 (g/m^3), and a hardness of 0.75 (mhos). MoS_2 nanoparticles were synthesized using a hydrothermal process and described as follow. First, separate aqueous solutions of (7 mM) ammonium molybdate tetrahydrate ((NH4)6Mo7O24 · 4H2O; 99.98%) and (35 mM) thiourea (Both purchased from Sigma-Aldrich) were prepared. Next, the solutions were mixed together to obtain a total volume of 50 mL. The final solution was vigorously stirred for 20 minutes before it was transferred to a Teflon-lined stainless steel autoclave. The hydrothermal process was carried out at 180 °C for 15 h, after which the autoclave was cooled to room temperature and the black powder of MoS_2 was collected. The MoS_2 powder was centrifuged and washed three times with deionized water and ethanol. The powder was dried at 60 °C for 2 h. MoS_2

nanoparticles prepared thus had the following properties: a spherical shape with a nominal diameter of 100 (nm), density of 5.06 (g/m^3), and a hardness of 1.5 (mhos) [101].

The surfactants used in this study were Oleic acid and Polyvinylpyrrolidone (both purchased from Sigma Aldrich). Oleic acid is a surfactant containing a hydrophilic hydroxyl end group and an organophilic alkyl chain [36]. PVP is a non-ionic polymer that contains a strongly hydrophilic molecule that can attach easily to materials in solution [95]. Figure 3.1 shows a schematic for the chemical structure of OA and PVP.

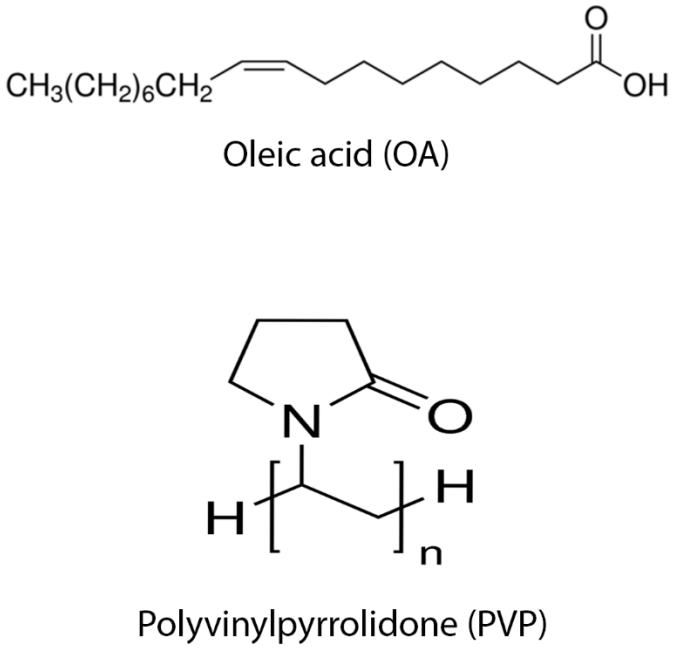

Figure 3.1 Schematic of the chemical structures of Oleic acid (OA) and Polyvinylpyrrolidone (PVP), that were chosen as surfactants.

In this study, the concentration of the nanoparticle additives in oil was chosen to be 1% by weight for each nanoparticle sample, based on the recommendation from studies on a variety of materials additives [10], [26], [27], [33], [89]. The particles added without any surfactant were sonicated for 60 minutes. For the formulations using Oleic acid as a

surfactant the samples were prepared by mixing 1% of weight Oleic acid to the PAO 1%wt nanoparticles solutions and sonicating the particles for 120 minutes. For the formulations using PVP as a surfactant, the samples were prepared as follows. Nanoparticles and PVP were added to the distilled water in the ratio of 3:1 by weight. The solution was subsequently sonicated for 30 minutes, followed by drying in an oven at 60° C for two hours. The resulting dry nanoparticles were added to the oil and sonicated for 60 minutes.

3.3.2Methods:

3.3.2.1 Dynamic light scattering

Extant research demonstrates that the agglomeration of nanoparticles tends to occur when they are added to in oil. Once agglomeration occurs, the particles size keeps changing. For a better estimate of the nominal particle size in solution, the size distribution of dispersed nanoparticles in PAO was measured by dynamic light scattering (DLS) (Malvern ZetaSizer Nano ZS). The theory underlying the measurements of the Zetasizer are based on effects of Brownian motions of nanoparticles on Rayleigh light scattering data to determine the size of a particle/molecule in solution. [67][102]. DLS data represents the hydrodynamic diameter distribution of the particles in solution and was collected at 15 minutes intervals over a space of 1 hour and the data. This corresponds to the typical friction and wear testing times.

3.3.2.2 Friction and wear testing

For the friction and wear experiments, a custom-built reciprocating ball-on-flat microtribometer that can produce a microscale (apparent area ~1000 μm^2) multi-asperity contact was used [71]. A schematic of the microtribometer major components is shown in Figure 3.2. A probe with a specific radius is placed at the end of a crossed I-beam structure,

which is lowered using a linear stage to apply a desired normal load to the sample. For this study, a SiC probe (4 mm diameter, hardness = 9 mohs, v = 0.19, E = 415 GPa), and an AISI 8620 steel substrate (4.5 mohs hardness) were used. The average substrate surface roughness (Ra) was approximately 0.06 μm as measured by Zygo NewView 7100 non-contact profilometrey over a scan area of 0.47 mm × 0.35 mm.

The normal and the friction (lateral) forces in the microtribometer are measured using semiconductor strain gages on the cantilevers. Friction forces can be resolved to approximately ±5 μN and normal forces to approximately ±15 μN. The signal from the normal load is monitored and used in a simple proportional-integral (PI) feedback loop to maintain the desired normal force regardless of any slope or waviness in the surface of the sample. The desired sample is affixed to another stage set perpendicular to the beam, which provides linear motion. An appropriate amount of the formulated oil was dropped to a fresh substrate surface prior conducting each test. A new SiC probe was used for each friction and wear test.

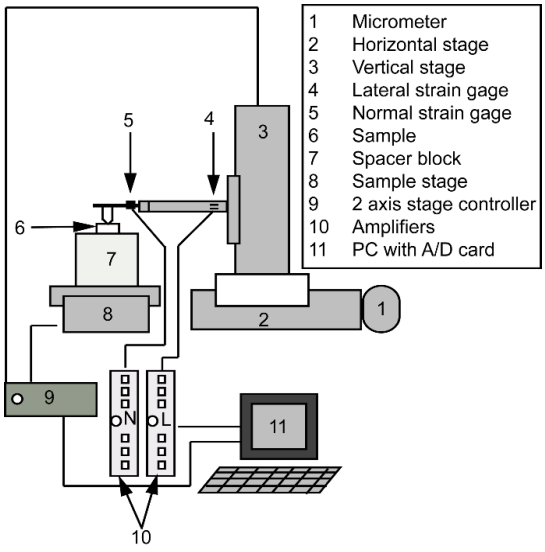

Figure 3.2 Schematic of Microtribometer used for friction and wear tests.

To evaluate the coefficient of friction the applied normal load was increased linearly from 0 to 2000 mN, for a specific sliding distance of 25 mm at a speed of 1 mm/s. Based on these parameters, the maximum Hertzian contact pressure was estimated to be 1.2 GPa, and the lubrication regime was boundary lubrication. The lateral force was recorded continuously along with the normal load for each test, providing a coefficient of friction. Five replicates were conducted for each condition, and the average coefficient of friction values were reported along with the 90% confidence interval. In order to obtain wear response, a reciprocating sliding wear test was performed against the SiC probe at a constant load of 5400 mN (maximum Hertzian force of 1.8 GPa) for 200 cycles, a stroke length of 8 mm, and a stroke speed of 10 mm/s. Two replicates were conducted for each sample. After each test, the sample surface was cleaned with isopropyl alcohol wipes and wear track depth were measured using Zygo profilometer. An average wear depth was reported from five measurements along each wear track and data reported as an average of 10 measurements (from two tests) along with a 90% confidence interval. Note that the test condition consisting of base oil with no additives was used as a control.

An FEI Quanta-250 Scanning Electron Microscope (FESEM) was used to obtain high-resolution images of wear tracks, and an Oxford Aztec energy-dispersive X-ray analysis was used to perform point analysis of the wear track and adjacent regions for evidence of any tribofilm formation. Backscattered images were analyzed for further tribofilm analysis with an accelerating voltage 10 kV and spot size 4 A.U. for all cases.

3.4. Results and Discussion

The results are presented and discussed in the following three sections. First, we describe the results related to reducing agglomeration of nanoparticle additives when dispersed in base oil. Next, we describe the friction behavior of the nanoadditives, followed by the results of the stable nanoadditives on wear behavior.

3.4.1 Dispersion of nanoparticles in oil:

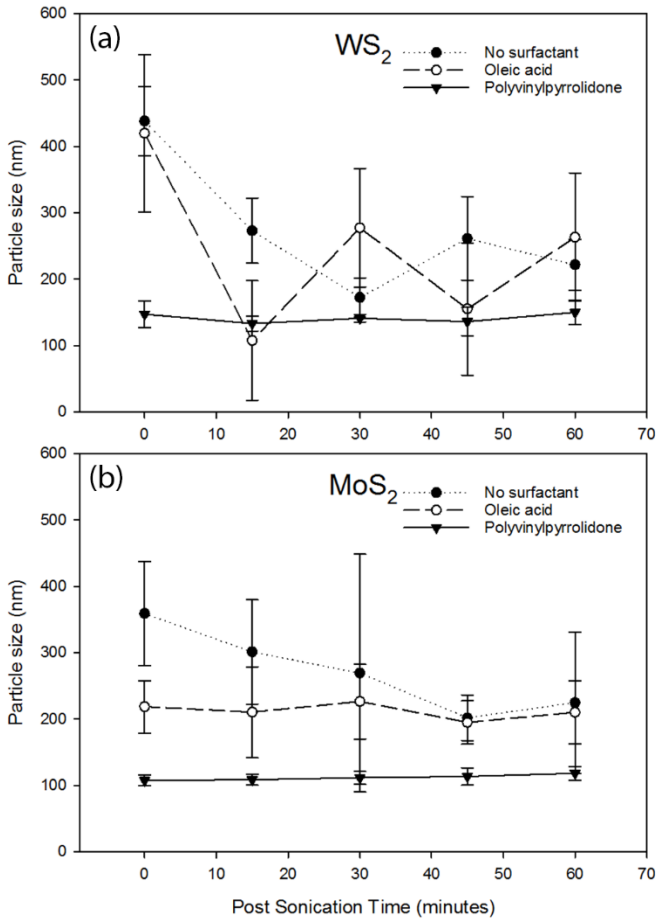

Figure 3.3 Dynamic light scattering (DLS) data are showing the average hydrodynamic diameter of (a) WS_2, (b) MoS_2, nanoparticles in PAO dispersed using different surfactants.

Figure 3.3 shows the average particle size as a function of post sonication time for the two nanoparticle additives and surfactants. The use of particles without surfactant resulted in initially high particles size (350 – 420 nm) and a gradual decrease over the testing duration with sizes of about 200 nm at 60 minutes. However, the absence of surfactants did lead to a very high variability in the particle size, suggesting unstable dispersion. For both particles, dispersing with PVP provided the lowest and most stable particle size for the testing duration. The stable particle size was around 150 nm and 100 nm for WS_2 and MoS_2 nanoparticles for the testing duration used. OA was less effective in reducing agglomeration as compared to PVP and by the 60 minutes mark, did not show appreciable improvements compared to the condition without surfactant. OA as a surfactant was more effective in the case of MoS_2 with a particle size of 200 nm but not as effective as PVP. However, the variability in the particle size was quite high compared to PVP. This variability was even more apparent in the case of WS_2.

Overall, while the addition of Oleic acid as well as treating the nanoadditives by PVP can form a layer on the nanoparticle surface and contribute to an increased diameter, the data suggest that agglomeration is the greater contributor to the increased diameters observed. This is supported by the fact that the observed diameters for particles with surfactants were lower than that of particles without surfactant. Furthermore, despite the fact that the amount by weight of PVP in the oil formulations for both particles was less than that of Oleic acid, the PVP dispersion technique showed lower particle size, thus pointing to agglomeration effects being the primary phenomenon being captured by the DLS data. In addition, visual impaction confirmed that the dispersion did not settle, thus eliminating this as a possible

reason for observing reduced particle size. Consequently, the dispersion technique using PVP contribute to effective agglomeration reduction and the most stable dispersion. We speculate that the difference in chemical structure of the surfactants contribute to the difference in their impact on agglomeration. The hydrophobic chain interactions of PVP combined with its effectiveness in forming surface films appear to lead to lower surface energy compared to the interactions of the non-polar ends of OA.

3.4.2: Friction behavior

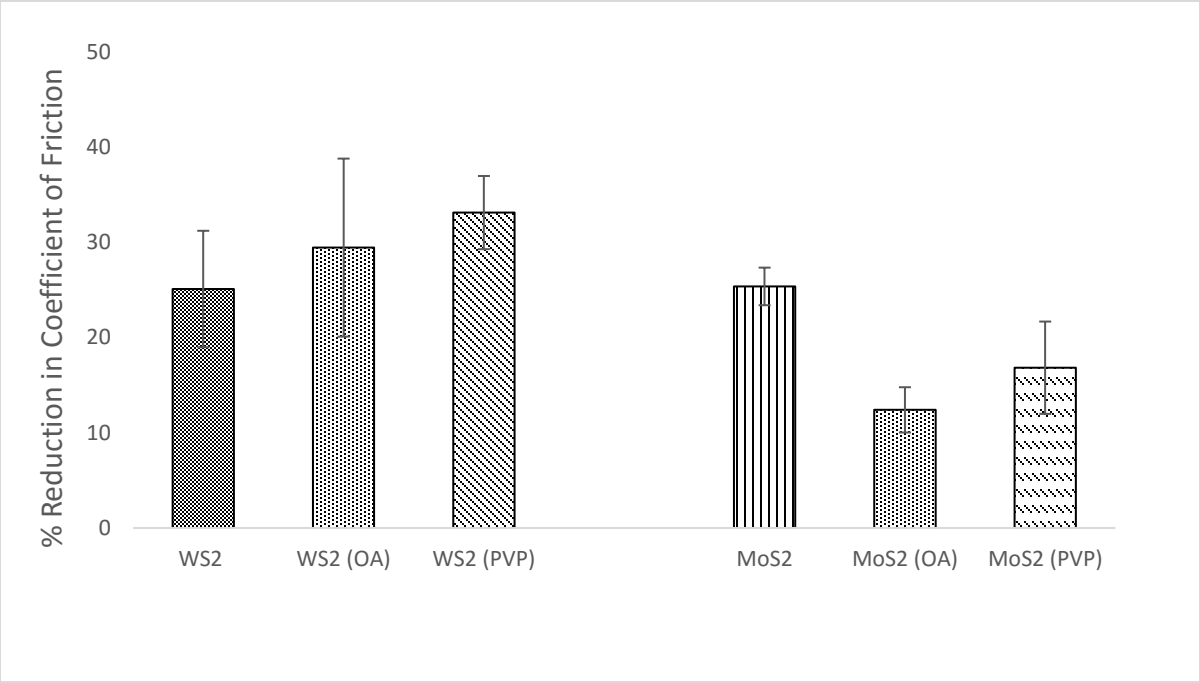

Figure 3.4 A comparison of the reduction in coefficient of friction exhibited by the various dispersion techniques for WS_2 and MoS_2 nanoparticles. Reductions are expressed as percentages with respect to the coefficient of friction observed in a base oil condition. Average values are shown along with 90% confidence intervals.

Figure 3.4 compares the reduction in coefficient of friction observed for the formulations of nanoparticle additive samples, relative to the coefficient of friction of the

neat base oil (PAO). All formulations exhibited a friction reduction with reductions ranging from 12% to 33%. When compared to the base oil, the average reduction using WS_2 particles with no surfactants was 25%. Additionally, the addition of Oleic acid showed a 29% reduction, while there was a 33% reduction using the PVP treatment for the WS_2 particles. There were high amounts of variability in friction reduction across the dispersion methods for WS_2, suggesting that the observed reductions are comparable among dispersion conditions, even though the average reduction in friction using the PVP treatment was the highest. As such, it appears that agglomeration reduction of the WS_2 nanoparticles can result in modest gains in friction performance under the specified testing conditions.

Friction tests of oil samples containing MoS_2 nano additives in base oil demonstrated lower levels of friction reduction compared to WS_2 nanoparticles due to the fact that WS_2 resists deformation in nanoscale more than to MoS_2 [103]. The measured average reduction percentage using MoS_2 added to lubricant without surfactant was 25%. In addition, the Oleic acid technique showed a 12% reduction on average, while there was a 16% reduction using the PVP treatment. MoS_2 nanoparticles dispersed in lubricant without surfactant had the best friction reduction compared to the other two techniques. The data indicates that agglomeration reduction of MoS_2 nanoparticle additives was not a requirement for a good friction reduction results.

Overall, the nanoadditives in this study reduced the coefficient of friction compared to the neat base oil. These results suggest that the WS_2 particles reduce friction by providing avenues for rolling friction rather than sliding friction. Reduced agglomeration (using PVP) enhances the ball bearing effect, thus providing lower friction compared to conditions where agglomeration occurs (no surfactant). MoS_2 particles appears to provide friction reduction by

the traditional shearing of planes. This explains why conditions where agglomeration is present provides better friction reduction compared to the conditions where MoS_2 is separated into individual particles.

3.4.3: Wear behavior

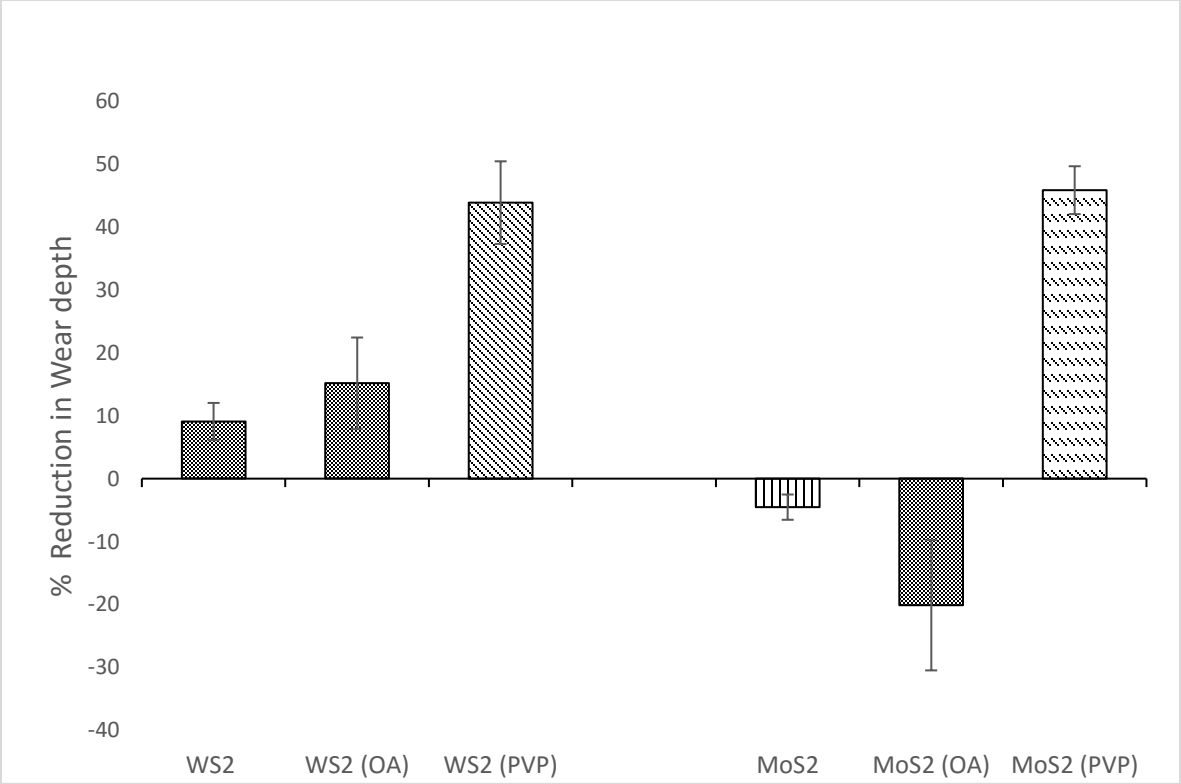

Figure 3.5 A comparison of the reduction in wear exhibited by the various dispersion techniques for WS_2 and MoS_2 nanoparticles. Reductions are expressed as percentages with respect to the wear observed with just the base oil. Positive values indicate improved wear performance, whereas negative values indicate poorer performance. Average values are shown along with 90% confidence intervals.

Figure 3.5 shows the results of the wear tests using WS_2 and MoS_2 nano additives and different dispersion techniques. Results shown are reductions in wear scar depths for each formulation compared to the wear depth observed using base oil. Positive values indicate

improved wear performance, whereas negative values indicate poorer performance compared to the wear depth observed with base oil only. The changes on the wear behavior varied from -22% to 45%, indicating that the nano additives could lead to an increase or decrease in the wear scar depth compared to the base oil and depending on the nanomaterial and the dispersion method used. Figure 3.6 shows representative wear scar particles for the various nanomaterial additives and dispersion conditions.

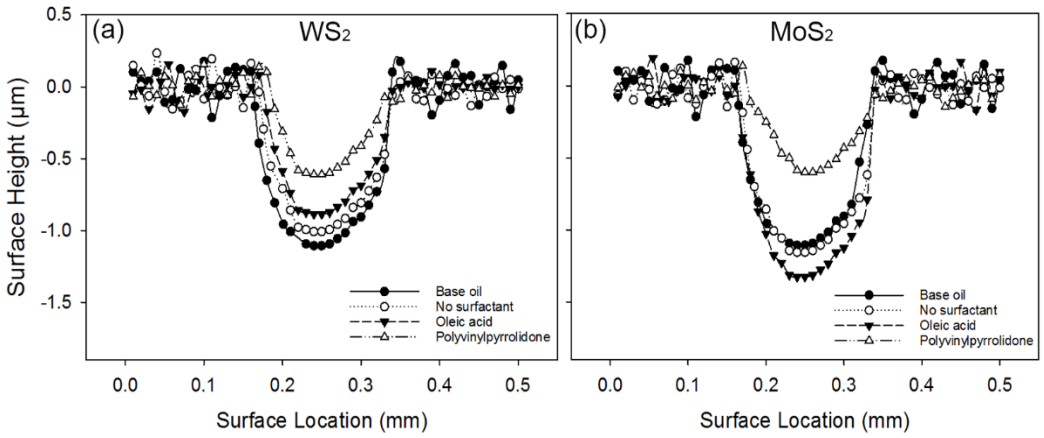

Figure 3.6 Representative wear scar profiles of different test conditions.

WS_2 nanoparticles exhibited a relative wear reduction in all of the tested dispersion techniques. For example, when compared to the base oil, the average reduction percentage observed using no surfactants was 9%. Treatment with Oleic acid technique yielded a 15% wear reduction, while treatment with PVP resulted in a 43% reduction. When taken together with the DLS data in Figure 3.3 (a), these results show that reducing agglomeration and enhancing dispersion stability promote increased wear resistance in the case of WS_2 nanoparticles.

The MoS_2 nanoadditives in base oil demonstrated different wear behavior than that of WS_2. The average wear reduction for MoS_2 when added to lubricant without surfactant was

approximately -5%, meaning that the wear scar depth increased by 5% when MoS_2 was added to the base oil. In addition, treatment with Oleic acid increased wear depth by 20% compared with the base oil. In contrast, the treatment with PVP, which as shown in Figure 3.3 (b), had the lowest and most stable particles size, resulted in a 45% wear scar depth reduction compared with base oil. This result suggests that agglomeration reduction of the nanoadditives alleviate the tribological behavior of the lubricant independent of the hardness of the tested nanomaterial. Reducing agglomeration and improving the dispersion of WS_2 and MoS_2 exhibited a comparable wear reduction of about 45%. We believe that increased abrasive wear via third body interactions occurred when the dispersion contained more agglomerated particles such as the conditions for MoS_2 nanoparticles when dispersed without surfactant and with Oleic acid. The lower hardness of WS_2 nanoparticles compared to MoS_2 mitigates this third body effect.

A primary interpretation of the nano additives behavior in boundary lubrication is that the small particles fill the valleys of the surface asperities and increases the real contact area, the nano additives then help share the load subjected to the surface asperities and reduce wear. We investigated substrate surfaces lubricated with nanoparticles treated by PVP, and without surfactant to better identify the prevailing mechanism of wear reduction. Figure 3.7 shows representative SEM images and EDS spectra of the wear tracks from the tests using the nanoparticles with and without PVP.

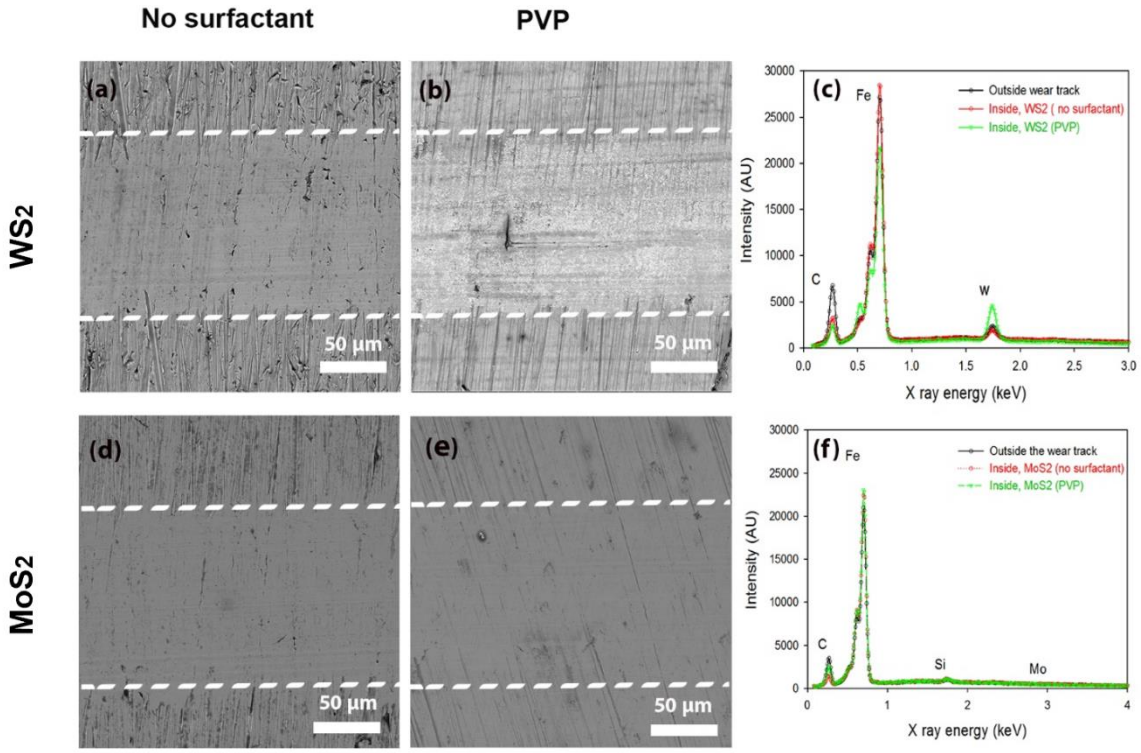

Figure 3.7 Scanning Electron Microscope (SEM) images of wear tracks on a steel substrate from sliding tests against a diamond probe of wear track. (a) WS_2 as additives, (b) WS_2 treated by PVP. Dotted lines indicate the edges of the wear track. (c) EDS data for WS_2 nano additives from regions inside and outside the wear tracks. The Figure demonstrates a lack of any particles or particle-based film formation when no surfactant used, and adhered W materials to the surface forming a layer of particles or particle-based film when the additives treated by PVP. (d) MoS_2 as additives, (e) MoS_2 treated by PVP. (f) EDS data for the different MoS_2 nano additives from regions inside and outside the wear track, showing lack of any particles or particle-based film formation.

Figure 3.7 (a), shows the SEM image of the wear track of the surface lubricated with 1%WS_2 dispersed without surfactant. It demonstrates an existence of abrasive wear via plastic deformation that changed the surface topography of the wear track region. In contrast, Figure 3.7 (b), demonstrates fewer changes in the surface topography inside the wear track when WS_2 nanoparticles were treated by PVP. Figure 3.7 (b) also shows a lighter color inside the wear track suggesting the existence of material layers other than steel. This layer could be

debris from the contact surfaces, or nano additives embedded in the surface. Figure 3.7 (c), shows the chemical analysis of the unworn and worn surfaces for WS_2 additives with and without PVP. EDS data identified a higher peak intensity of W particles present inside the wear track when lubricated using WS_2 treated by PVP. This is evidence of nanoparticle-based film formation on the wear track surface that could be the cause of the higher wear reduction observed for this dispersion condition. EDS did not show the presence of sulfur on the wear surface. It is possible that the surface treatment of WS_2 using PVP has made the WS_2 bonds weaker and easier for W particles to get separated and subsequently adhered to the steel surface. Further testing is necessary to confirm these possibilities.

Figures 3.7 (e) and (f) compares MoS_2 nanoparticles dispersed with and without PVP. Wear tracks of the substrates show evidence of abrasive wear via ploughing similar to that observed using WS_2. PVP treated nanoparticles resulted in less surface deformation on the worn surface and fewer changes on the surface topography between the outside and inside wear track regions. Analyses of SEM images and EDS data for the substrates reveal no evidence of any MoS_2 nanoparticle-based material on any of the wear tracks. MoS_2 materials combine high hardness with low shear strength, and it appears that the particles remained free in the oil. This suggests the mechanism of wear reduction for well dispersed MoS_2 in the boundary lubrication condition is via load support of rolling nanoparticles rather than the formation of a tribofilm. The agglomeration reduction and homogeneous particle dispersion help to make particles roll more, and contribute to the wear reduction.

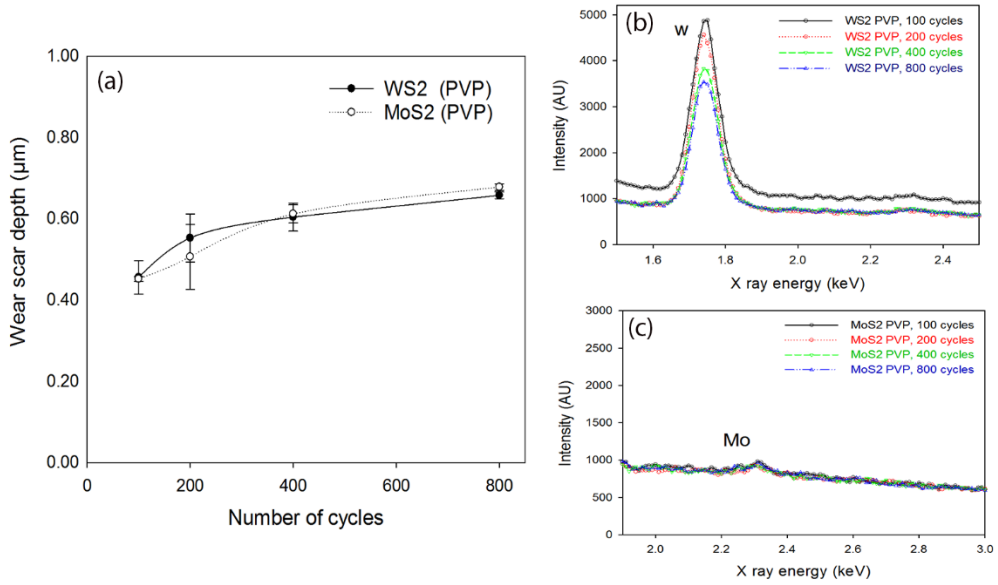

Figure 3.8(a) Wear scar depth data in µm for different cycles when WS_2 and MoS_2 nanoparticles treated by PVP. (b) EDS data for WS_2 nano additives treated by PVP from regions inside the wear tracks for different cycles, showing a decrease in the adhered W materials to the surface formed a layer of particles when the number of cycles increase. (c) EDS data for the MoS_2 nano additives treated by PVP from regions inside the wear tracks for different cycles, showing lack of any particles or particle-based film formation.

We were expecting that WS_2 nanoparticles treated by PVP would provide a higher level of relative wear reduction compared to MoS_2 because of the tribofilm formed on the substrate. But as demonstrated in Figure 3.4 the wear reduction in WS_2 was equivalent to MoS_2 nano additives treated by PVP, which we believe reduced wear via nanoscale rolling effect. This equivalency maybe due to the lack of durability of the WS_2 a tribofilm, or MoS_2 may have formed a film as well but was removed before the 200 cycles used in the previous analyses (Figure 3.5). In order to investigate these possibilities, we performed wear depth measurements and EDS analyses at 100, 200, 400, and 800 cycles at the same load.

Figure 3.8 (a) shows variations of the average wear scar depth as a function of sliding cycles. The wear scar depth increased sharply at first, but then gradually increased between

200 and 800 cycles. WS_2 showed a slightly lower wear rate increase compared to MoS_2. At 800 cycles WS_2 exhibited a slightly lower wear scar depth. However, this difference is minimal. Figure 3.8 (b) shows EDS data for the wear tracks for various sliding cycles for WS_2 with PVP. A decrease in intensity of the adhered W materials to the surface is observed as the number of cycles increase. The data suggest that tribofilm formation is the dominant wear reduction mechanism when WS_2 with PVP is used, and this tribofilm is susceptible to wear. This explains why it did not show higher relative wear reduction compare with MoS_2 PVP. Despite the tribofilm wear susceptibility, it is quite durable film under the tested conditions. Figure 3.8 (c) shows the intensity level of Mo particles inside the wear track regions on the substrates surfaces when were lubricated by MoS_2 with PVP for different wear track cycles. The data shows a lack of any particles or particle-based film formation when MoS2 with PVP nano additives were used. The data reinforces the load sharing via rolling and that there was not any tribofilm formed under this condition.

3.5. Conclusions

This study tested different suspension techniques for WS_2 and MoS_2 nanoparticles to enhance agglomeration reduction and improve the particles dispersion in PAO. Subsequently, the tribological behavior exhibited by the various dispersion techniques of the nanoparticles in boundary lubricant regime was investigated. The nanoparticles were dispersed using the following techniques: 1) 60 minutes sonication without using a stabilizing agent, 2) 60 minutes sonication with 1% of weight Oleic acid (OA), and 3) functionalizing the nanoparticles using PVP (3:1 ratio of nanoparticles to PVP). The dispersion conditions using PVP showed the most stable particle size and homogeneous mixture dispersion for both nanoparticles.

Friction studies showed that nanoparticle agglomeration reduction and the homogeneity of the suspension do not significantly impact the friction reduction behavior of the lubricant. Reciprocating wear experiments showed that for our test conditions, both WS_2 and MoS_2 nano additives showed maximum wear depth reduction (45%) when using the PVP surface treatment compared to base oil. The wear results confirmed the significance of minimizing agglomeration and promoting high dispersion, in enabling favorable wear resistance under boundary lubricant conditions. Further analysis using SEM of the wear surfaces showed that a tribofilm formation was the primary wear reduction mechanism for WS_2 particles treated by PVP, whereas in the case of MoS_2 the mechanism was load sharing via particles rolling and/or sliding. Overall, the study demonstrates that stabilizing the dispersion of WS_2 and MoS_2 nanoparticle and minimizing agglomeration will improve wear resistance under boundary lubricant conditions.

CHAPTER 4. INVESTIGATING THE MICROPITTING PERFORMANCE OF COPPER OXIDE AND TUNGSTEN CARBIDE NANOFLUIDS UNDER BOUNDARY LUBRICATION

*Yosef Jazaa, Sougata Roy and Sriram Sundararajan**

Department of Mechanical Engineering, Iowa State University, Ames IA 50011, USA

Manuscript in preparation for submission to "Tribology International"

4.1 Abstract

This paper investigated the potential of copper oxide (CuO) and tungsten carbide (WC) nanofluids in enhancing micropitting life of AISI 8620 steel. The nanofluids consisted of 1% nanoparticles by weight and 1% by weight of Oleic acid surfactant in Polyalphaolefin (PAO). Rolling contact fatigue tests were conducted using a micropitting test rig (MPR). Both the nanofluids exhibited increased micropitting life compared to the base oil. Tungsten carbide nanofluids showed significantly higher micropitting resistance behavior than the copper oxide nanofluids under the boundary lubrication regime. Analysis of the surfaces showed different mechanisms to inhibit micropitting and wear for the two nanofluids-the tungsten carbide nanofluid formed a tribofilm whereas the CuO nanofluids tended to fill surface cracks with the nanoparticles.

4.2 Introduction

Recent studies showed that adding nanoparticles such as Cu, CuO, Al_2O_3, graphene, SnO_2, TiO_2, and CNT to base oil can improve the lubricant viscosity, thermal conductivity, heat transfer and other rheological properties [21], [104]–[110] of the lubricants. Several studies have also demonstrated that the addition of nanoparticles can enhance the friction behavior and

wear resistance of a range of lubricants [9], [14], [88], [111]–[113]. Studying the impact of adding nanoparticles to oils and lubricants to enhance rolling contact fatigue life is gaining significance in academia and industry. Minondo et al. investigated the rolling contact fatigue life using two lubricants with and without additive, their results showed that polytetrafluoroethylene (PTFE) additives is more effective in TMP05 synthetic oil than in SN-350 [20]. Y. Zhang et al. showed that changing the concentration of nano-Cu additives result in varying improvements in the rolling contact fatigue behavior [114]. Micropitting is one of the crucial rolling contact fatigue failure mode which is responsible for component failure of wide range of machineries working under high load and low speed (i.e. boundary lubrication regime) such as wind turbines, agricultural machineries and earth moving equipment[115], [116][4], [43]. Micropitting is a surface initiated failure mode [117], [118], so there is a great possibility that a stable nanofluid (lubricants with nanomaterial additives) can impact micropitting life significantly. The literature suggests that lower sized nanoparticles, ranging from 30 nm to 300 nm in diameter, reduce friction and wear the most on contact surfaces[8], [30]. Dispersing nanoparticles in lubricant is a challenging process as it tends to agglomerate due to strong Van der Waal forces [5], [24], [94]. Dispersion of nanoparticle additives can be improved by sonication, the addition of a surfactant or a contribution of the two [24], [25], [46], [73]. The choice of specific dispersion method is typically determined by the nanomaterials used and their surface energy.

In this study, nanofluids prepared using CuO and WC nanoparticles and Oleic acid as a surfactant were used as lubricants in ring-on-ring type rolling contact fatigue test rig and their performance were compared to that of base oil. Rolling contact fatigue is a complex failure phenome where several competing failure modes including cracking, micropitting, and wear,

can coexist and compete with each other. Analysis of surface damage evolution and surface analysis to elucidate mechanisms of one failure observed with the three nanoparticles were conducted and presented.

4.3 Experimental section

4.3.1 Substrate material

Experiments were conducted on carburized AISI 8620 steel which is a widely used material in drive train components. The samples were case carburized, subsequently ground and polished to achieve an average surface roughness level of 0.22 ±0.02 μm over a scan size of 1 mm × 0.6 mm.

4.3.2 Nanofluid preparation

The base oil used in this experiment was Polyalphaolefin (PAO), with the following specifications as reported by the manufacturer (Exxon mobile corporation): density 826 g/m^3 at 15° C, and viscosity 400 cSt at 40°C. The base oil lubricant did not have any additives. Commercially available CuO and WC nanoparticles were purchased from Zhengzhou Dongyao Nano Materials Co. Ltd. TEM images of the nanoparticles are showed in Figure 4.1.

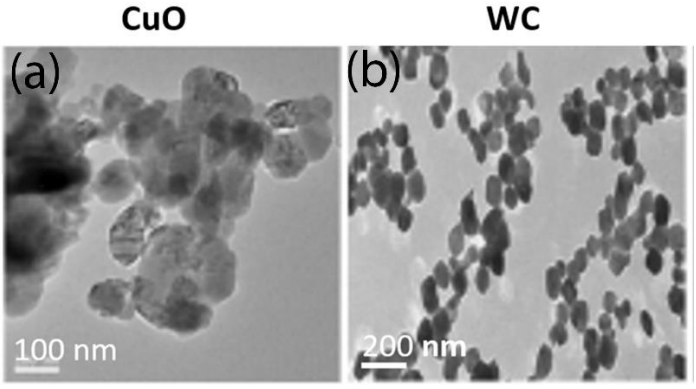

Figure 4.1 TEM images of (a) CuO and (b) WC nanoparticles.

Selected properties of the nanoparticles, as reported by the manufacturer are listed in Table 4.1. In order to better isolate the effect of the materials, the nominal size (100 nm) and shape (spherical) of the particles were selected to be comparable.

Table 4.1 Selected physical properties of the nanoparticles used in the study.

Nanoparticles	**Density (g/m^3)**	**Hardness mhos**	**Nominal diameter (nm)**	**Nominal shape**
CuO	6.4	3.5	100	Spherical
WC	15.63	7.5	100	Spherical

In this study, the concentration of the nanoparticles in oil was chosen to be 1% by weight based on recommendation from studies on a variety of additives[10,18-24]. The nanoparticles were dispersed in 150 ml oil using Oleic acid as a surfactant. The samples were prepared by mixing 1% Oleic acid by weight while sonicating the particles for 120 minutes. Oleic acid (CH3(CH2)7CH=CH(CH2)7COOH) is a surfactant containing hydrophilic hydroxyl and organophilic alkyl [36]. The hydrophilic end attaches to the nanoparticles and interactions between the alkyl ends are expected to result in reduced surface energy, which helps minimize agglomeration.

4.3.3 Nanofluid characterization

Extant research demonstrates that the agglomeration of nanoparticles tends to occur when they are added to in oil and once agglomeration occurs, the particles size keeps changing. For a better estimate of the nominal particle size in solution, the size distribution of dispersed nanoparticles in PAO was measured by dynamic light scattering (DLS) (Malvern ZetaSizer Nano ZS). The theory underlying the measurements of the Zetasizer is based on effects of Brownian motions of nanoparticles on Rayleigh light scattering data to determine the size of a

particle/molecule in solution [67], [102]. DLS data represents the hydrodynamic diameter distribution of the particles in solution DLS data was collected over a space of 1 hour following sample preparation. The reported nominal particle size was 100 nm, but the DLS data in Figure 4.2 shows that the average particle size in PAO range from about 200-250 nm for CuO and WC. This suggests that some agglomeration may be occurring for all particles. When CuO was dispersed with 1% OA to in PAO and sonicated for 120 minutes; the average particle size reduced to about 120 nm at 10 minutes post sonication time and increased to about 177 nm at 60 minutes post sonication time. Dispersing WC particles in PAO with 1% OA and sonication for 120 minutes resulted in average particle size 175 nm. Thus, the addition of Oleic acid helped to reduce agglomeration.

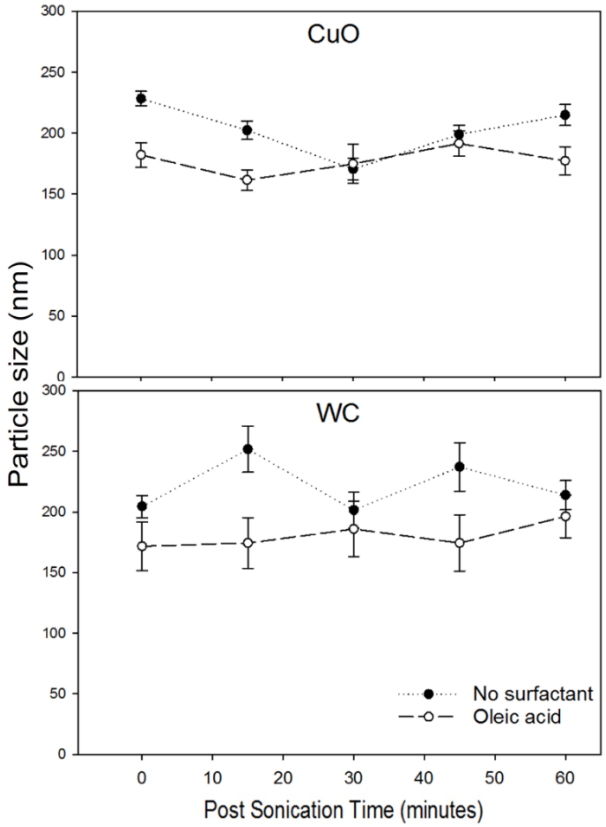

Figure 4.2 Nanoparticle sizes as a function of post sonication time before and after adding surfactant measured using DLS spectroscopy.

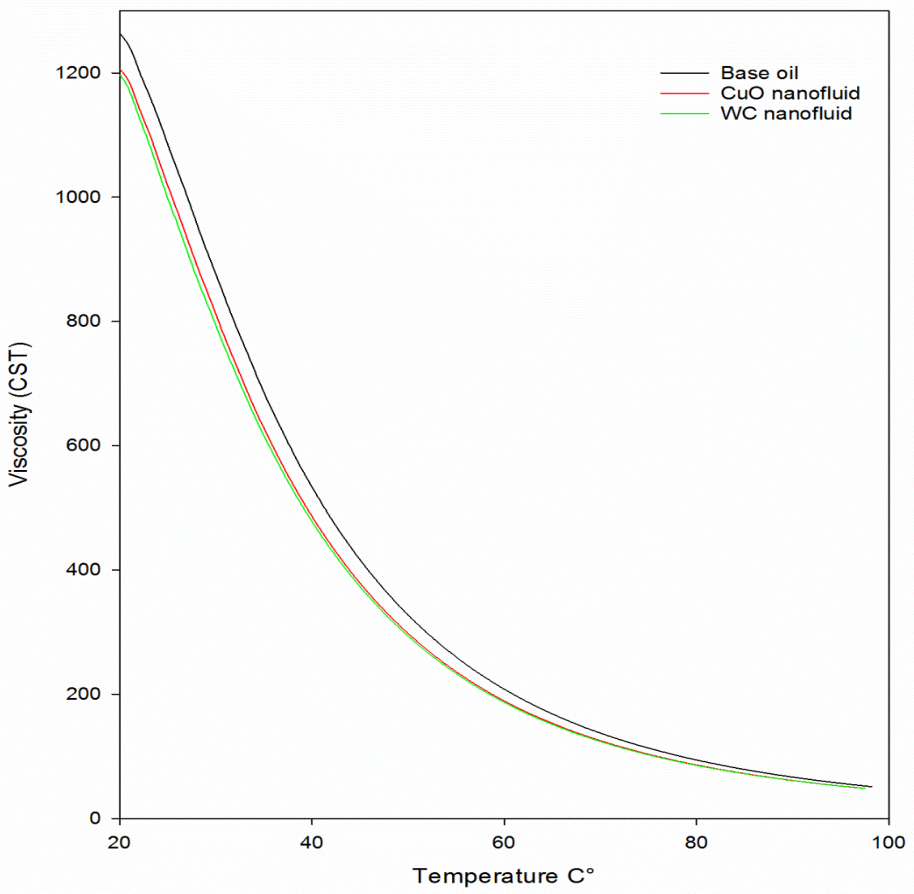

Figure 4.3 Viscosity vs Temperature response for used nanofluids.

Viscosity measurements of the lubricant formulations were accomplished using a TA Instruments ARES G2 stress control rheometer. The ARES-G2 rheometer is able to accurately measure the viscosity of oils with a dedicated actuator for deformation control, a torque Rebalance Transducer (TRT), and a Force Rebalance Transducer (FRT) for independent shear stress and normal stress measurements. The viscosity vs temperature response for all three fluids are showed in Figure 4.3. It can be observed that all three fluids had comparable viscosity response during a wide range of temperature. This is especially true at 80° C, which is the temperature of the lubricants in our rolling contact fatigue tests.

4.3.4 Rolling contact fatigue test

Rolling contact fatigue (RCF) tests were performed using a Micro Pitting Rig (MPR) by PCS instruments (London, UK). A schematic representation of the experimental setup is shown in Figure 4.4 (a). The MPR is a computer controlled disc-on-disc contact instrument in which a central roller (sample) is in contact with three harder counter face rings in a planetary configuration as shown in Figure 4.4 (b). The roller therefore experiences three contact cycles per revolution at a constant contact pressure. A chamfered roller with face-width 1mm (see Figure 4.4 c) was used for the tests performed in this study. The diameter for roller and rings were 12 mm and 54.15 mm respectively. The MPR utilizes a dip lubrication system, with the oil level 27.8 millimeters below the center of the roller and a sump volume of 150 milliliters. The unit is also temperature controlled to maintain the desired operating temperature of the lubricant sump. The speeds of the rings and rollers are controlled independently which allows different combinations of rolling and sliding contact. The relative amount of rolling and sliding is determined by the slide-to-roll ratio (SRR) and is defined as follows:

$$\text{SRR}\ (\%) = \frac{U_1 - U_2}{{}^1\!/_2 (U_1 + U_2)} \cdot 100 \qquad (4.1)$$

Where U_1 is the speed of the rings and U_2 is the speed of the roller. All tests were conducted using the conditions listed in Table 4.2. The normal load resulted in a maximum Hertzian contact pressure of 1.5 GPa.

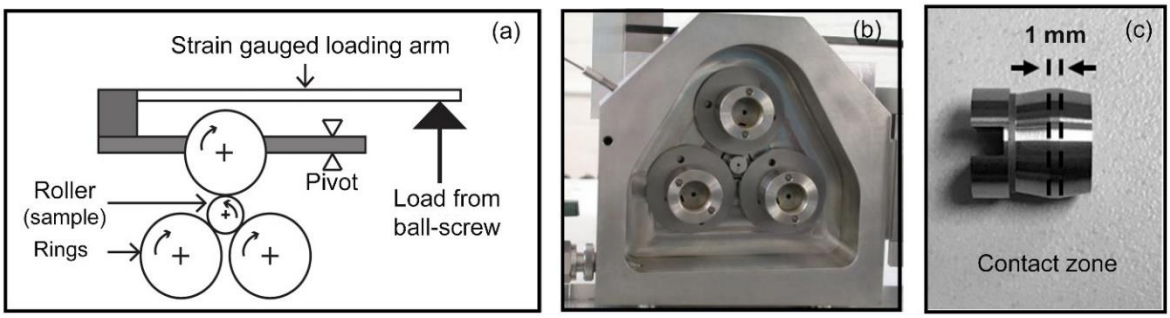

Figure 4.4 (a) Schematic diagram of micropitting test rig (MPR); (b) Experimental setup of roller and rings inside MPR chamber; (c) Image of the roller (test sample) showing the contact zone.

Table 4.2 Operating conditions for rolling contact fatigue (RCF) tests.

Test parameter	
Entrainment velocity (m/sec)	1.75
Slide to roll ratio (%)	20
Normal Load (N)	311
Maximum Hertzian contact pressure (GPa)	1.5
Lubricant sump temperature (°C)	80

Minimum oil film thickness (H_{min}) for the experiments was calculated using the Pan-Hamrock's equation mentioned below,

$$H_{min} = 1.714\, U^{0.694} G^{0.568} W^{-0.128} \quad (4.2)$$

where, U is dimensionless speed parameter, G is the dimensionless material parameter, and W is the dimensionless load parameter. The film thickness ratio (λ) was calculated using H_{min} and measured initial composite roughness (Rq) to verify tests were run under boundary lubrication. Based on the viscosity properties of the lubricants the lambda ratio (minimum oil film thickness) for base oil, CuO and WC nanofluids were 0.48 (237 μm), 0.46 (229 μm) and 0.46 (226 μm) respectively, confirming boundary lubrication conditions (lambda < 1).

An accelerometer attached to the instrument provides peak to peak (P/P) and center-line-

average (CLA) values of vibration due to crack propagation and surface deformation during RCF tests. All experiments were run up to 50 million contact cycles or till the system detected a P/P accelerometer signal of 10g, whichever occurred first. Each experiment was associated with a 2-min 'ramp-up' step where the test parameters were ramped to preset conditions (as mentioned in Table 4.2) for the upcoming fatigue step.

4.3.5 Micropitting quantization and characterization

Most of the studies conducted previously on micropitting utilize microscopic imaging to provide a qualitative evaluation of surface damage [48], [115], [117], [119], [120]. In this study, we attempted to capture evolution of micropitting quantitatively using analysis of data collected using white light non-contact profilometry. The RCF tests were interrupted periodically to obtain topographical data for roughness analysis and to quantify the amount of micropitting on the rollers. Depending on the RCF life of the samples, data was obtained after 0.1, 1, 5, 10, 20 million cycles and at the end of tests.

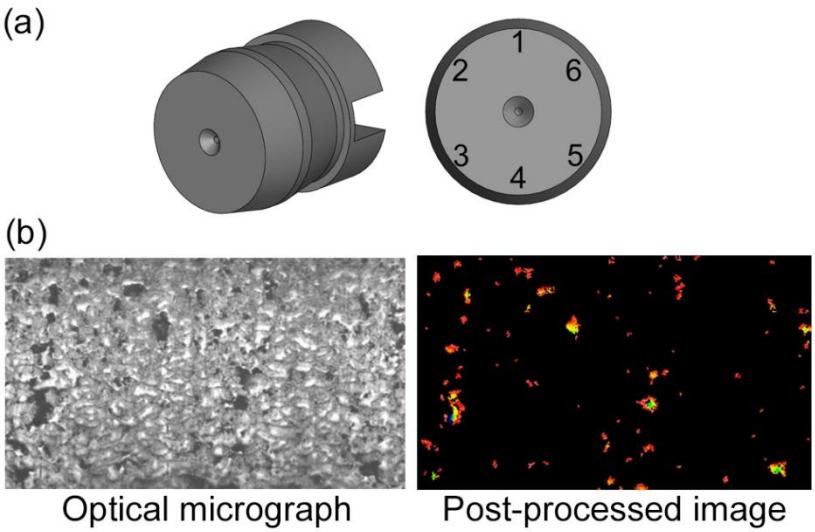

Figure 4.5 (a) Surface images were obtained at six locations around the sample circumference (b) Optical micrographs were converted to quantized maps of micropitted regions.

A Zygo NewView 7100 microscope with a white light interferometer was used to obtain topographical data from six different locations around the roller circumference (approximately 60° apart) as shown in Figure 4.5. Images from those six locations were post-processed using the Zygo's texture analysis software to detect micropitted regions. A surface region with depth greater than 1 μm and an area above 25 μm^2 was considered to be a micropit. Subsequently, the total micropitted area (expressed as percentage) was calculated by calculating averaging data from the six circumferential locations. A FEI Quanta-250 Scanning Electron Microscope (FESEM) was used to obtain high resolution images of micropits using Back Scattered Electron topography mode with an excitation voltage of 10 kV. The FESEM was also used to conduct chemical analysis via energy dispersive spectroscopy (EDS) of the contact surface including the micropitted regions.

4.4 Results

4.4.1 Rolling contact fatigue (RCF) test results

Samples subjected to tests with the three different lubricants exhibited very distinct RCF life as shown in Table 4.3. Both the CuO and WC nanofluids showed improved rolling contact fatigue life compared to the base oil. It can be observed that the samples had the lowest RCF life under base oil lubricated conditions and maximum life under WC lubricated conditions.

Table 4.3 RCF life of test samples

Sample		RCF life
Base oil	Test 01	19.9 million
	Test 02	23.2 million
CuO nanofluid	Test 01	25.3 million
	Test 02	43 million
WC nanofluid	Test 01	>50 million
	Test 02	>50 million

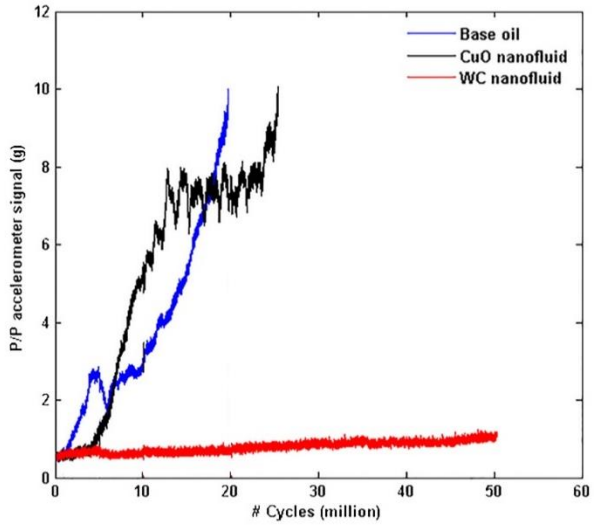

Figure 4.6 Peak-to-peak (P/P) accelerometer signal response as a function of RCF test cycles under different lubricating conditions.

Figure 4.6 shows representative graphs of the evolution of P/P accelerometer signals from the tests conducted using different lubricating fluids. In case of base oil, the signal exhibited an increasing trend from the start of the tests. For the CuO nanofluid case, the accelerometer signal increased steadily after about 4 million cycles and up to 10 million cycles, after which the signal remained stable upto 20 million cycles and increased again subsequently. In case of WC nanofluid, the increasing slope of the signal was significantly lower and almost negligible compared to other two cases. Consequently, the roller didn't reach an accelerometer

signal level of 10g even at 50 million cycles in the case of the WC nanofluid.

Figure 4.7 shows the surface evolution of roller surfaces during rolling contact fatigue tests. The base oil condition results in visible damage across the contact surface even at 5 million cycles, and throughout the test till failure. In case of the CuO nanofluid, the surface exhibits some damage at 5 million cycles with increasing lateral cracks and pits up to failure. However, they are not as widespread as the base oil condition. Tungsten carbide nanofluid showed significantly improved performance in protecting roller surface during RCF tests, with a low number of visible cracks and puts up to 50 million cycles. These visual observations correlate qualitatively with the changes in the accelerometer signal as a function of test contact cycles.

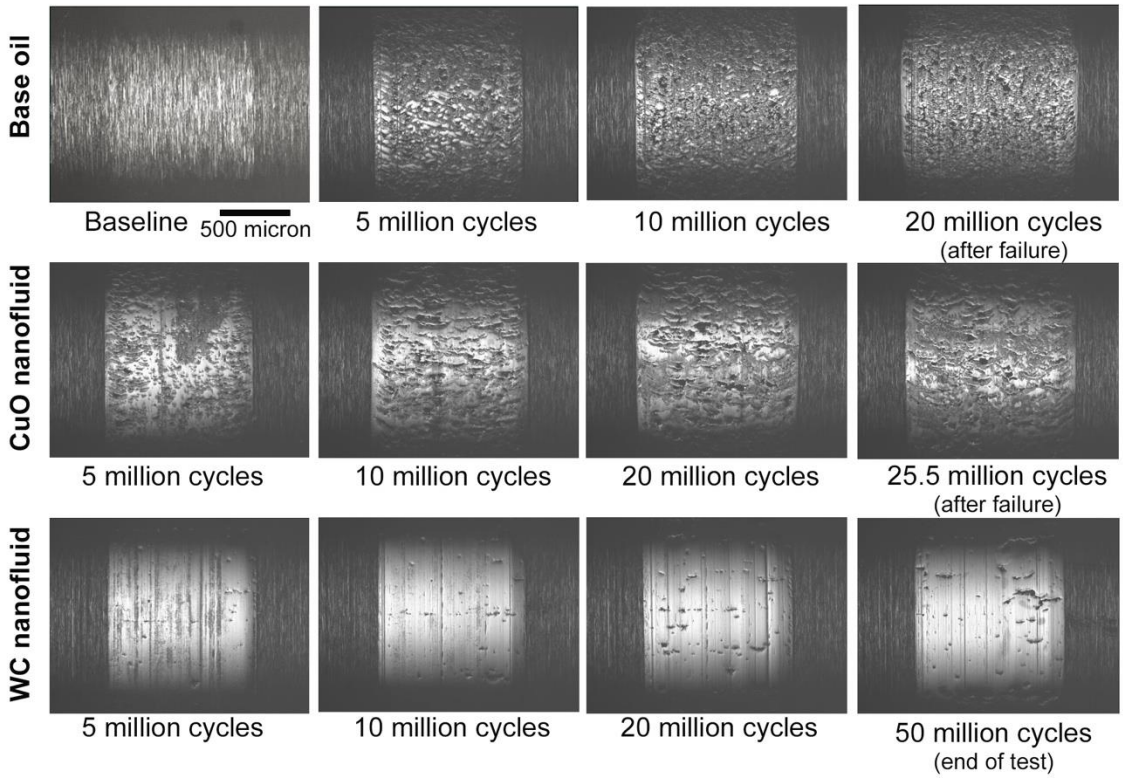

Figure 4.7 Optical micrographs showing surface evolution on roller samples.

4.4.2 Micropitting percentage during tests

Figure 4.8 shows the evolution of quantified micropitting area under different lubricating conditions. Tests conducted using the base oil resulted in the highest micropitted area. The increasing area with increasing contact cycles correlates well with the increasing accelerometer data. In case of CuO nanofluids, the micropitted area increased initially after which it dropped after 10 million cycles. The accelerometer signal showed a relative flat response during this period. After 20 million cycles although micropitting didn't propagate significantly, formation and propagation of surface cracks lead to increase in P/P accelerometer signal. In case of WC nanofluids, the micropitted area was significantly lower compared to other two lubricating fluids.

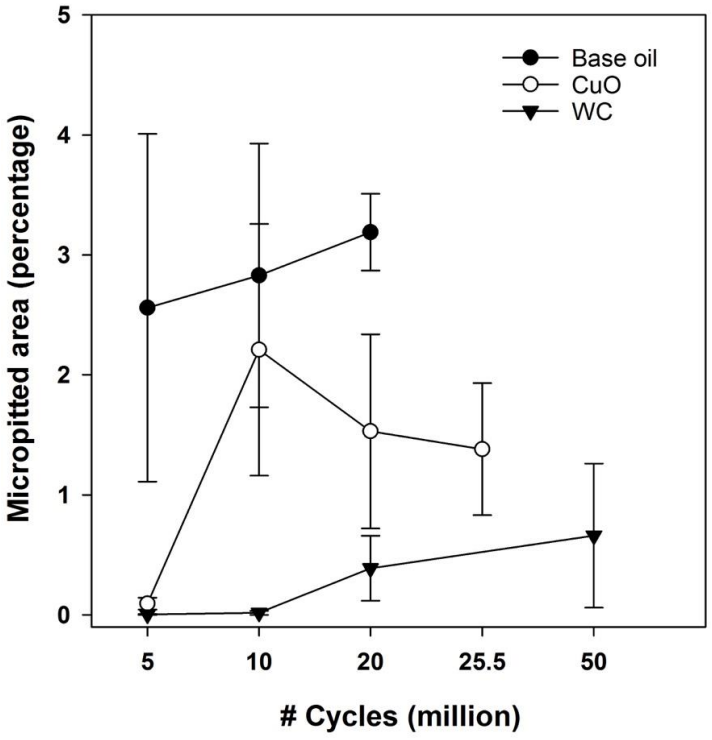

Figure 4.8 Evolution of microppiting during RCF tests under different lubrication conditions.

Roller facewidths were tracked during RCF tests to capture the occurrence of wear. A widening of the facewidth of the contact area would occur due to synergistic impact of abrasive wear, cracking and micropitting on roller surface. As shown in Figure 4.9, the facewidth showed an increasing trend in all three cases with increasing RCF cycles. The wear exhibited by the samples tested with just base oil is the most severe and correlates with the high levels of micropitting and cracking observed (Figure 4.7 and 4.8). In the case of the CuO nanofluid, the wear was less than that obtained in the base oil case, but still significant. This wear may have contributed to lower levels of micropitting area observed in these samples (Figure 4.8) due to reduced pit depths resulting from overall surface wear. In case of WC, the facewidth increase was insignificant compared to that observed with the other two fluids, suggesting less abrasive wear, crack formation and micropitting on the surface.

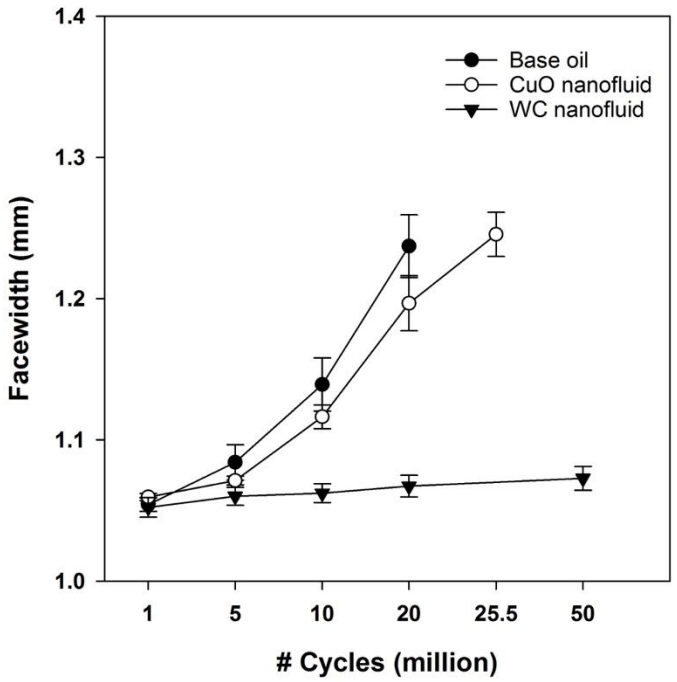

Figure 4.9 Figure 4.10 Evolution of test sample facewidth during RCF tests under different lubricating fluids.

4.4.3 SEM and chemical analysis

Figure 4.10 (a) shows representative SEM images of the contact surfaces of the samples after 1 million RCF cycles. Roller surfaces were observed using energy dispersive X-ray spectroscopy to understand the mechanism providing for the different nanofluids. Figure 4.10 (b) shows the X-ray spectra collected from the whole region of each of the images. All three pectra overlap each other.

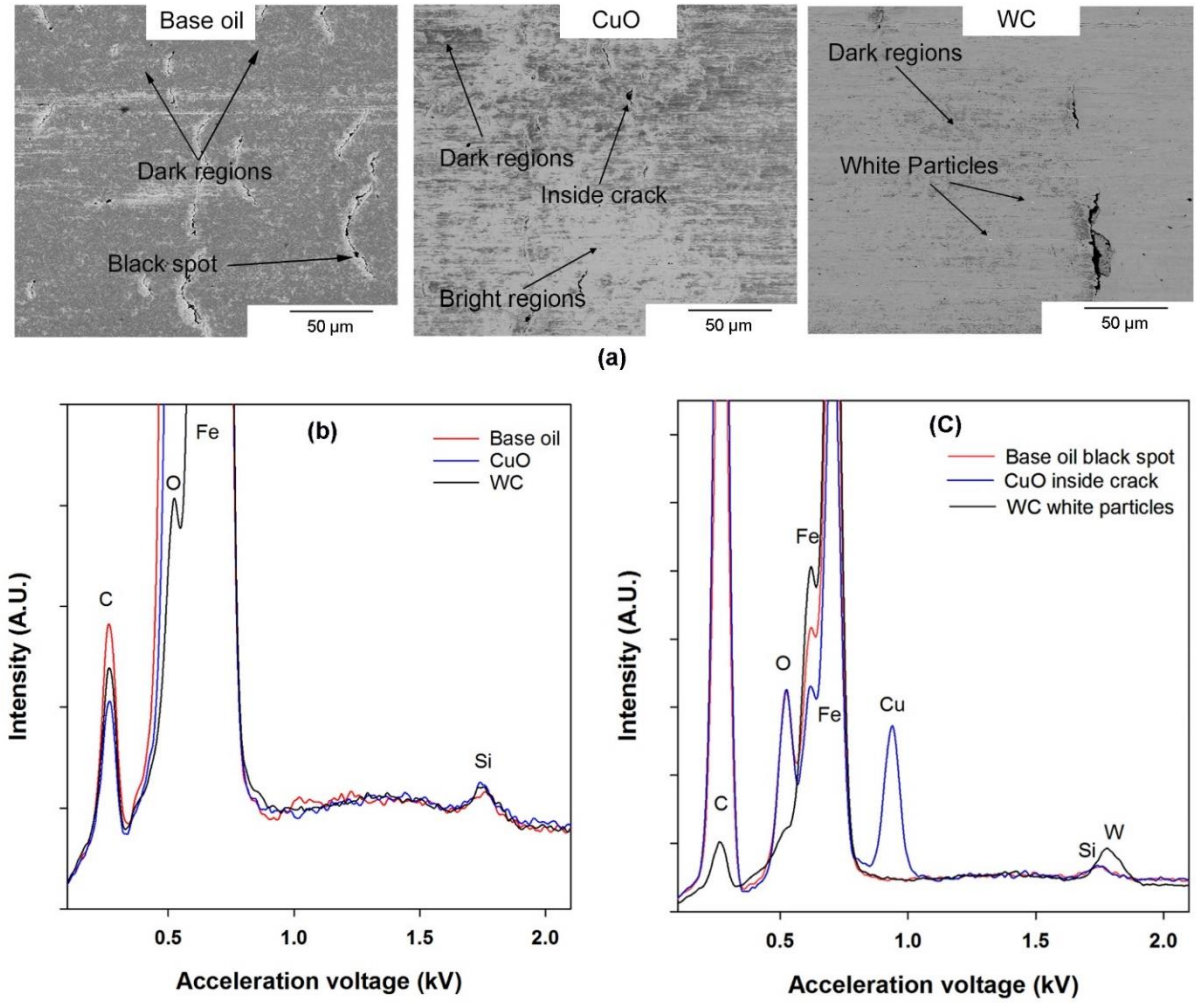

Figure 4.11 (a) SEM images of regions within the contact zone of test samples after 1 million RCF cycles. EDS data from (b) entire region in the SEM images, and (c) specific areas as indicated.

showing no formation of any tribofilms or discrete regions of WC or CuO nanoparticles on the sample surface. Figure 4.10 (c) shows EDS data from specific areas on the sample surfaces. In all three cases, the darker regions appear to be heavily more oxidized zones and brighter zones are less oxidized. It can be observed that in case of CuO lubricated case, although there was no trace of nanoparticles from the data collected from the whole region, CuO was observed inside the cracks. In case of the WC lubricated condition, traces of WC nanoparticles were found on the sample surface as well as inside the cracks.

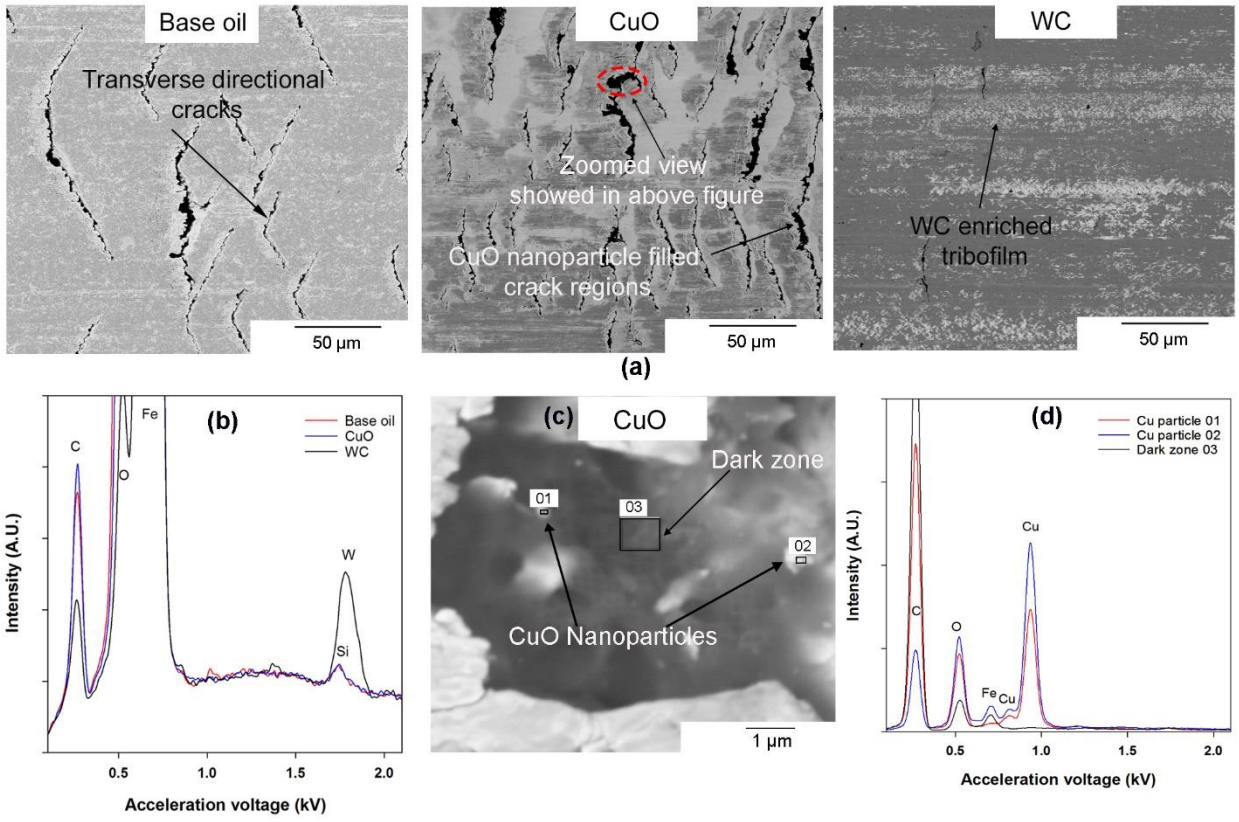

Figure 4.12 (a) SEM images of regions within the contact zone of all samoples after 5 million RCF cycles. (b) EDS data from entire region of the SEM images. (c) High magnification SEM image of a crack of sample lubricated with CuO nanofluid and (d) corresponding EDS data, showing CuO particles inside the crack.

Figure 4.11 shows SEM images and EDS spectra of the sample surfaces after 5 million cycles. Figure 4.11(b) shows comparison of the EDS spectra taken from the entire region of the images. The absence of a strong Cu signal confirmed that there was no trace of CuO nanoparticles on the contact surface. On the other hand, the discretely observed WC nanoparticles after 1 million cycles had accumulated on the sample surface over the time and formed a WC tribofilm after 5 million of RCF cycle. This helped protect the surface significantly from wear, cracking and micropitting. A crack location of the sample surface lubricated under CuO nanofluid was observed in high magnification (15000x) and is shown in Figure 4.11 (c). EDS data was collected from three regions of this crack and is shown in Figure 4.11 (d). The existence of CuO nanoparticles was captured at zone 01 and zone 02 inside the crack. Thus, the agglomeration of CuO nanoparticles inside cracked regions helped mitigate crack and micropit growth, leading to better RCF life compared to that of base oil.

The differences in the protection mechanism between the two nanofluids is further supported by the traction coefficient data collected during the RCF tests, shown in Figure 4.12. It can be observed that the traction coefficient was significantly lower in the case of WC nanofluids due to formation of tribofilm. The traction coefficient for the base oil and CuO nanofluid were comparable, due to the lack of any film formation.

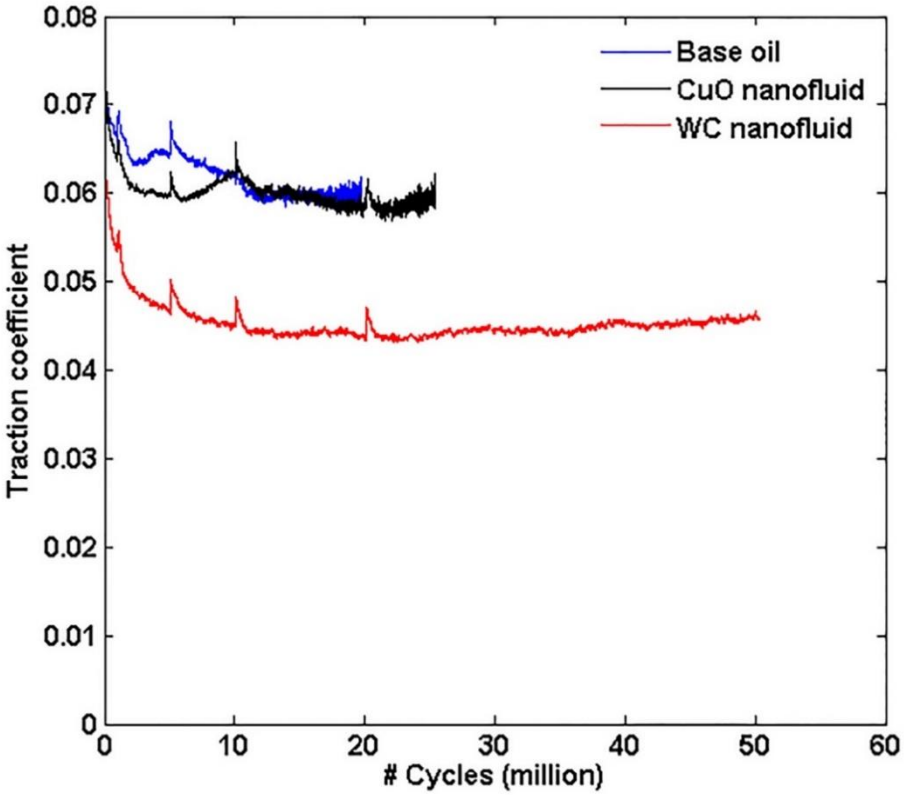

Figure 4.13 Traction coefficient response under different lubricating fluid conditions.

Secondary electron images were collected at the end of every test and representative images are shown in Figure 4.13. The amount of surface damage in terms of cracks and micropits are significantly high for base oil and CuO nanofluid cases. Existence of WC tribofilms were detected in some regions on the sample surface even after 50 million RCF cycles. But in some regions the films were not present. This suggests that the tribofilm formed after 5 million cycles undergoes abrasion during the higher RCF cycles, or that the particles are physically absorbed onto the surface.

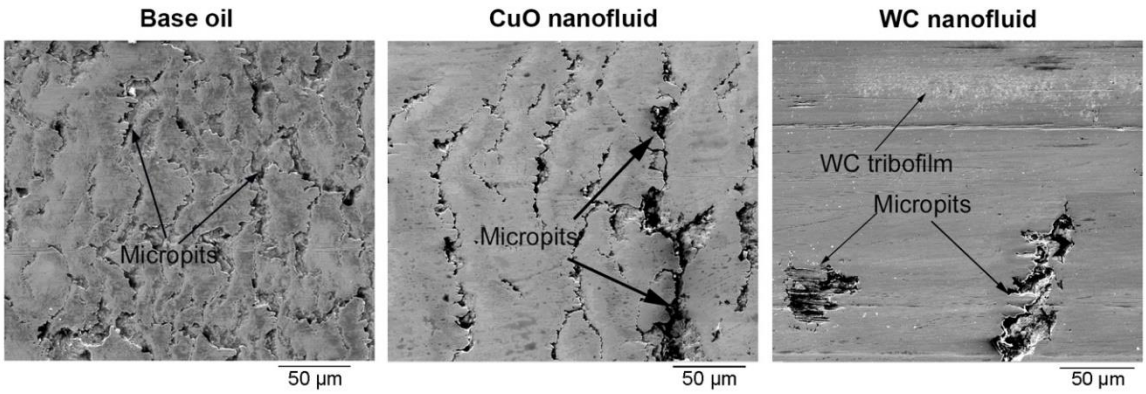

Figure 4.14 Secondary electron images of test sample surfaces at the end of RCF test cycles.

4.5 Conclusions

The study investigated the potential of nanoparticle additives to lubricants in protecting carburized steel surfaces from micropitting under boundary lubrication condition. The results can be summarized as:

- Both CuO and WC nanoparticles showed improved performance in protecting sample surface from micropitting and both nanofluids showed better RCF life compared to base oil.
- WC nanofluids showed significantly superior performance in reducing micropitting, wear and traction coefficient on sample surface with samples showing excellent resistance to micropitting beyond 50 million contact cycles.
- In case of CuO nanofluids, the nanoparticles filled the cracked regions to some extent and this delayed the propagation of micropitting after certain number of cycles. In case of WC nanofluids, the nanoparticles formed a tribofilm on the sample surface.

Overall, the findings provide valuable input for engineering the next generation lubricating fluids for drivetrain components in a wide range of applications under low lambda conditions ranging from agricultural equipment to the wind energy sectors.

Acknowledgement

The authors would like to thank Matt Smeeth from PCS Instruments for his help with sample preparation, Warren Straszheim in the Materials Analysis and Research Laboratory (MARL) for help with SEM imaging. Partial funding for this work was provided by John Deere Product Engineering Center in Waterloo, Iowa and Iowa State University.

CHAPTER 5. CONCLUSIONS

In this study, the impact of adding nanoparticle additives to lubricants on their tribological performance was investigated under boundary lubrication conditions. To better understand the friction and wear reduction mechanism different nanoparticle additives of comparable nominal diameter were added to a Polyalphaolefin (PAO) base oil to evaluate tribological response. Before conducting tribological testing, the agglomeration nd stability of the dispersion were evaluated. The significant results and observations with respect to each research objective are summarized below.

Influence of surfactants on the tribological behavior of nanoparticle additives under boundary lubrication conditions

The study investigated the tribological impact of adding different nanoparticle additives to oil in boundary condition lubricant regime, including looking at factors that minimize nanoparticle agglomeration. Boundary condition lubricant regime refers to application areas of high load and low operating speed mainly observed in drivetrain components (gears and bearings).

The results showed that adding 10 % Oleic acid to (CuO, WS_2, WC) nanoparticle additives while sonicating the particles for 30 minutes reduced the particle size the most out of the methods studied. Adding 1% Oleic acid while sonicating the particles for 120 minutes produced a more uniform dispersion; whereas WS_2 exhibited much higher variation in particle size despite the addition of surfactants presumably due to its high surface energy

compared to the other particles.

Friction experiments under boundary lubrication showed that adding nanoparticles can enhance lubricity to varying degrees (10 – 20 %) under different dispersion conditions. Minimizing agglomeration did not seem to be a necessary contribution for friction reduction.

Reciprocating wear experiments showed that agglomeration reduction and homogeneous particles dispersion contribute to the wear reduction by increasing the true contact area and reducing shear forces on the roughness asperities.

These conditions showed wear depth reduction of about 63% for CuO and 50% for WC as compared to the wear depth observed for the base oil. WS_2 nanoparticle results were not considered in this study due to high variability of nanoparticle dispersion stability even though they exhibited a 42% wear reduction in wear depth when tested with 10% OA and 30 minutes sonication.

The effect of agglomeration reduction on the tribological behavior of WS_2 and MoS_2 nanoparticle additives in boundary lubrication regime

This study tested different suspension techniques for WS_2 and MoS_2 using the following techniques: 1) 60 minutes sonication without using a stabilizing agent, 2) 60 minutes sonication with 1% of weight Oleic acid (OA), and 3) functionalizing the nanoparticles. The nanoparticles which were functionalized using Polyvinylpyrrolidone showed stable particles size and homogeneous mixture dispersion.

Friction studies showed that nanoparticle agglomeration reduction and the homogeneity of the suspension do not significantly impact the friction reduction behavior of the lubricant. Reciprocating wear experiments showed that for our test conditions, both WS_2

and MoS_2 nano additives showed maximum wear depth reduction (45%) when using the PVP surface treatment compared to base oil. The wear results confirmed the significance of minimizing agglomeration and promoting high dispersion, leading to favorable wear resistance under boundary lubricant conditions. Further analysis using SEM of the wear surfaces showed that a tribofilm formation was the primary mechanism for WS_2 particles treated by PVP whereas in the case of MoS_2, load sharing via particles rolling and/or sliding to help increasing contact area.

Investigating the micropitting performance of copper oxide and tungsten carbide nanoparticle additives under boundary lubrication

The study investigated the potential of nanoparticle additives to lubricants in protecting carburized steel surfaces from micropitting under boundary lubrication condition. The results can be summarized as:

- Both CuO and WC nanoparticles showed improved performance in protecting sample surface from micropitting and both nanofluids showed better RCF life compared to base oil.
- WC nanofluids showed significantly superior performance in reducing micropitting, wear and traction coefficient on sample surface with samples showing excellent resistance to micropitting beyond 50 million contact cycles.
- In case of CuO nanofluids, the nanoparticles filled the cracked regions to some extent and this delayed the propagation of micropitting after certain number of cycles. In case of WC nanofluids, the nanoparticles formed a tribofilm on the sample surface.

Overall, the findings from the dissertation provide valuable input for engineering the next generation lubricating fluids of drivetrain components for a wide range of applications under low lambda conditions ranging from agricultural equipment to the wind energy sectors. Future scope of the study could include an impact in the automobile, renewable energy and machining industries. The addition of nanoparticles to common base oils is a promising approach towards enhancing friction and wear resistance.

REFERENCES

[1] B. Bhushan, *Introduction to tribology / Bharat Bhushan.* New York: New York : John Wiley, 2002.

[2] R. Chattopadhyay, *Green tribology, green surface engineering, and global warming / Ramnarayan Chattopadhyay.* Materials Park, Ohio : ASM International, 2014.

[3] P. Dougherty, "Synthesizing in situ Friction and Wear with ex situ Surface Metrology to Provide Post-mortem Tribological Analysis : Experiments and Modeling," 2016.

[4] K. Holmberg and A. Erdemir, "Influence of tribology on global energy consumption, costs and emissions," *Friction*, vol. 5, no. 3, pp. 263–284, 2017.

[5] M. Asrul, N. W. M. Zulkifli, H. H. Masjuki, and M. A. Kalam, "Tribological properties and lubricant mechanism of nanoparticle in engine oil," *Procedia Eng.*, vol. 68, pp. 320–325, 2013.

[6] J. Williams, "Engineering Tribology," *Oxford Univ. Press*, vol. 427, p. 488, 1994.

[7] S. Sasaki, "Tribological Properties of Ionic Liquids," Y. Kondo and J. Kadokawa, Eds. Rijeka: InTech, 2013, p. Ch. 5.

[8] S. R. Makhsin, K. A. Razak, R. Noordin, N. D. Zakaria, and T. S. Chun, "The effects of size and synthesis methods of gold nanoparticle-conjugated MαHIgG4 for use in an immunochromatographic strip test to detect brugian filariasis.," *Nanotechnology*, vol. 23, no. 49, p. 495719, 2012.

[9] V. Zin, F. Agresti, S. Barison, L. Colla, A. Gondolini, and M. Fabrizio, "The synthesis and effect of copper nanoparticles on the tribological properties of lubricant oils," *IEEE Trans. Nanotechnol.*, vol. 12, no. 5, pp. 751–759, 2013.

[10] Y. Y. Wu, W. C. Tsui, and T. C. Liu, "Experimental analysis of tribological properties of lubricating oils with nanoparticle additives," *Wear*, vol. 262, no. 7–8, pp. 819–825, 2007.

[11] Z. J. Zhang, D. Simionesie, and C. Schaschke, "Graphite and Hybrid Nanomaterials as Lubricant Additives," *Lubricants*, vol. 2, no. 2, pp. 44–65, 2014.

[12] V. Zin, F. Agresti, S. Barison, L. Colla, and M. Fabrizio, "Influence of Cu, TiO2 Nanoparticles and Carbon Nano-Horns on Tribological Properties of Engine Oil," *J. Nanosci. Nanotechnol.*, vol. 15, no. 5, pp. 3590–3598, 2015.

[13] L. Rapoport *et al.*, "Behavior of fullerene-like WS2 nanoparticles under severe contact conditions," *Wear*, vol. 259, no. 1–6, pp. 703–707, 2005.

[14] F. Chiñas-Castillo and H. a. Spikes, “Mechanism of Action of Colloidal Solid Dispersions,” *J. Tribol.*, vol. 125, no. JULY 2003, p. 552, 2003.

[15] M. Kalin, J. Kogovšek, and M. Remškar, “Mechanisms and improvements in the friction and wear behavior using MoS 2 nanotubes as potential oil additives,” *Wear*, vol. 280–281, pp. 36–45, 2012.

[16] F. Zhao, Z. Bai, Y. Fu, D. Zhao, and C. Yan, “Tribological properties of serpentine, La(OH)3 and their composite particles as lubricant additives,” *Wear*, vol. 288, no. 2012, pp. 72–77, 2012.

[17] Z. Jia, Y. Xia, X. Shao, and S. Du, “Synthesis, characterization and tribological behavior of oleic acid-capped core-shell lanthanum borate-SiO\n 2\n composites,” *Ind. Lubr. Tribol.*, vol. 66, no. 1, pp. 1–8, 2014.

[18] N. Nunn, Z. Mahbooba, M. G. Ivanov, D. M. Ivanov, D. W. Brenner, and O. Shenderova, “Tribological properties of polyalphaolefin oil modified with nanocarbon additives,” *Diam. Relat. Mater.*, vol. 54, no. 1, pp. 97–102, 2015.

[19] D. Guo, G. Xie, and J. Luo, “Mechanical properties of nanoparticles: basics and applications,” *J. Phys. D. Appl. Phys.*, vol. 47, no. 1, p. 013001, 2014.

[20] E. F. Rico, I. Minondo, and D. G. Cuervo, “Rolling contact fatigue life of AISI 52100 steel balls with mineral and synthetic polyester lubricants with PTFE nanoparticle powder as an additive,” *Wear*, vol. 266, no. 7–8. pp. 671–677, 2009.

[21] A. Ghadimi, R. Saidur, and H. S. C. Metselaar, “A review of nanofluid stability properties and characterization in stationary conditions,” *Int. J. Heat Mass Transf.*, vol. 54, no. 17–18, pp. 4051–4068, 2011.

[22] D. Kim and L. A. Archer, “Nanoscale organic-inorganic hybrid lubricants,” *Langmuir*, vol. 27, no. 6, pp. 3083–3094, 2011.

[23] M. Venkataraman, “The effect of colloidal stability on the heat transfer characteristics of nanosilica dispersed fluids,” p. 93, 2005.

[24] Y. Hwang *et al.*, “Production and dispersion stability of nanoparticles in nanofluids,” vol. 186, pp. 145–153, 2008.

[25] Z. Haddad, C. Abid, H. F. Oztop, and A. Mataoui, “International Journal of Thermal Sciences A review on how the researchers prepare their nano fl uids,” vol. 76, pp. 168–189, 2014.

[26] L. Joly-Pottuz, F. Dassenoy, M. Belin, B. Vacher, J. M. Martin, and N. Fleischer, “Ultralow-friction and wear properties of IF-WS2 under boundary lubrication,” *Tribol. Lett.*, vol. 18, no. 4, pp. 477–485, 2005.

[27] L. Zhang, G. Liu, G. bin Yang, S. Chen, B. yun Huang, and C. fu Zhang, “Surface adsorption phenomenon during the preparation process of nano WC and ultrafine cemented carbide,” *Int. J. Refract. Met. Hard Mater.*, vol. 25, no. 2, pp. 166–170, 2007.

[28] F. Chiñas-Castillo and H. A. Spikes, “Mechanism of Action of Colloidal Solid Dispersions,” *J. Tribol.*, vol. 125, no. 3, p. 552, 2003.

[29] C. Altavilla, M. Sarno, P. Ciambelli, A. Senatore, and V. Petrone, “New ‘chimie douce’ approach to the synthesis of hybrid nanosheets of MoS2 on CNT and their anti-friction and anti-wear properties.,” *Nanotechnology*, vol. 24, no. 12, p. 125601, 2013.

[30] D. Guo, G. Xie, and J. Luo, “Mechanical properties of nanoparticles: basics and applications,” *J. Phys. D. Appl. Phys.*, vol. 47, no. 1, p. 13001, 2014.

[31] W. Zhang, D. Demydov, M. P. Jahan, K. Mistry, A. Erdemir, and A. P. Malshe, “Fundamental understanding of the tribological and thermal behavior of Ag-MoS 2 nanoparticle-based multi-component lubricating system,” *Wear*, vol. 288, pp. 9–16, 2012.

[32] L. L. Zhang, J. P. Tu, H. M. Wu, and Y. Z. Yang, “WS2 nanorods prepared by self-transformation process and their tribological properties as additive in base oil,” *Mater. Sci. Eng. A*, vol. 454–455, pp. 487–491, 2007.

[33] P. Xu, Z. Li, X. Zhang, and Z. Yang, “Increased response to oxidative stress challenge of nano-copper-induced apoptosis in mesangial cells,” *J. Nanoparticle Res.*, vol. 16, no. 12, 2014.

[34] M. Ratoi, V. B. Niste, and J. Zekonyte, “WS2 nanoparticles - potential replacement for ZDDP and friction modifier additives,” *RSC Adv.*, vol. 4, no. 41, pp. 21238–21245, 2014.

[35] M. Kole and T. K. Dey, “Effect of aggregation on the viscosity of copper oxide-gear oil nanofluids,” *Int. J. Therm. Sci.*, vol. 50, no. 9, pp. 1741–1747, 2011.

[36] W. Zhang *et al.*, “Tribological properties of oleic acid-modified graphene as lubricant oil additives,” *J. Phys. D. Appl. Phys.*, vol. 44, no. 20, pp. 1–4, 2011.

[37] L. Wu, Y. Zhang, G. Yang, S. Zhang, L. Yu, and P. Zhang, “Tribological properties of oleic acid-modified zinc oxide nanoparticles as the lubricant additive in poly-alpha olefin and diisooctyl sebacate base oils,” *RSC Adv.*, vol. 6, no. 74, pp. 69836–69844, 2016.

[38] Y. Gao, R. Sun, Z. Zhang, and Q. Xue, “Tribological properties of oleic acid — modified TiO 2 nanoparticle in water,” *Mater. Sci. Eng. A*, vol. 286, pp. 149–151, 2000.

[39] S. Q. a Rizvi, *A Comprehensive Review of Lubricant Chemistry, Technology, Selection and Design*. 2009.

[40] L. Rapoport *et al.*, “Friction and wear of fullerene-like WS2 under severe contact conditions: Friction of ceramic materials,” *Tribol. Lett.*, vol. 19, no. 2, pp. 143–149, 2005.

[41] G.-J. Lee, J.-J. Park, M.-K. Lee, and C. K. Rhee, “Stable dispersion of nanodiamonds in oil and their tribological properties as lubricant additives,” *Appl. Surf. Sci.*, pp. 10–13, 2016.

[42] P. Hansson and B. Lindman, “Surfactant-polymer interactions,” *Curr. Opin. Colloid Interface Sci.*, vol. 1, no. 5, pp. 604–613, 1996.

[43] G. Biresaw and K. L. Mittal, “Surfactants in Tribology.,” in *Surfactants in Tribology*, no. December, 2008, pp. 407–408.

[44] J. Feng, J. Mao, X. Wen, and M. Tu, “Ultrasonic-assisted in situ synthesis and characterization of superparamagnetic Fe3O4 nanoparticles,” *J. Alloys Compd.*, vol. 509, no. 37, pp. 9093–9097, 2011.

[45] Y. Rao, “Particuology Nanofluids : Stability , phase diagram , rheology and applications,” *Particuology*, vol. 8, no. 6, pp. 549–555, 2010.

[46] A. Ghadimi and I. H. Metselaar, “The influence of surfactant and ultrasonic processing on improvement of stability , thermal conductivity and viscosity of titania nanofluid,” *Exp. Therm. Fluid Sci.*, vol. 51, pp. 1–9, 2013.

[47] A. Hernández Battez *et al.*, “CuO, ZrO2 and ZnO nanoparticles as antiwear additive in oil lubricants,” *Wear*, vol. 265, no. 3–4, pp. 422–428, 2008.

[48] E. Lainé, A. V. Olver, and T. A. Beveridge, “Effect of lubricants on micropitting and wear,” *Tribol. Int.*, vol. 41, no. 11, pp. 1049–1055, 2008.

[49] H. Fissan, S. Ristig, H. Kaminski, C. Asbach, and M. Epple, “Comparison of different characterization methods for nanoparticle dispersions before and after aerosolization,” *Anal. Methods*, vol. 6, no. 18, pp. 7324–7334, 2014.

[50] N. Nunn, Z. Mahbooba, M. G. Ivanov, D. M. Ivanov, D. W. Brenner, and O. Shenderova, “Tribological properties of polyalphaolefin oil modified with nanocarbon additives,” *Diam. Relat. Mater.*, vol. 54, no. 1, pp. 97–102, 2015.

[51] R. Chou, A. H. Battez, J. J. Cabello, J. L. Viesca, A. Osorio, and A. Sagastume, “Tribological behavior of polyalphaolefin with the addition of nickel nanoparticles,” *Tribol. Int.*, vol. 43, no. 12, pp. 2327–2332, 2010.

[52] Y. Choi *et al.*, “Tribological behavior of copper nanoparticles as additives in oil,” *Curr. Appl. Phys.*, vol. 9, no. 2 SUPPL., pp. e124–e127, 2009.

[53] J. L. Viesca, A. Hernández Battez, R. González, R. Chou, and J. J. Cabello, “Antiwear properties of carbon-coated copper nanoparticles used as an additive to a polyalphaolefin,” *Tribol. Int.*, vol. 44, no. 7–8, pp. 829–833, 2011.

[54] R. D. Evans, G. L. Doll, C. H. Hager, and J. Y. Howe, “Influence of steel type on the propensity for tribochemical wear in boundary lubrication with a wind turbine gear oil,” *Tribol. Lett.*, vol. 38, no. 1, pp. 25–32, 2010.

[55] S. Zhou, L. Wang, and Q. Xue, “Controlling friction and wear of nc-WC/a-C(Al) nanocomposite coating by lubricant/additive synergies,” *Surf. Coatings Technol.*, vol. 206, no. 10, pp. 2698–2705, 2012.

[56] S. M. Alves, V. S. Mello, E. A. Faria, and A. P. P. Camargo, “Nanolubricants developed from tiny CuO nanoparticles,” *Tribol. Int.*, vol. 100, pp. 263–271, 2016.

[57] M. Ratoi, V. B. Niste, J. Walker, and J. Zekonyte, “Mechanism of action of WS2 lubricant nanoadditives in high-pressure contacts,” *Tribol. Lett.*, vol. 52, no. 1, pp. 81–91, 2013.

[58] R. Greenberg, G. Halperin, I. Etsion, and R. Tenne, “The effect of WS2 nanoparticles on friction reduction in various lubrication regimes,” *Tribol. Lett.*, vol. 17, no. 2, pp. 179–186, 2004.

[59] V. S. Jatti and T. P. Singh, “Copper oxide nano-particles as friction-reduction and anti-wear additives in lubricating oil,” *J. Mech. Sci. Technol.*, vol. 29, no. 2, pp. 793–798, 2015.

[60] M. Kreuzeder, M. D. Abad, M. M. Primorac, P. Hosemann, V. Maier, and D. Kiener, “Fabrication and thermo-mechanical behavior of ultra-fine porous copper,” *J. Mater. Sci.*, vol. 50, no. 2, pp. 634–643, 2014.

[61] D. S. Tordonato and A. D. Skaja, “Investigation of Molybdenum Disulfide and Tungsten Disulfide as Additives to Coatings for Foul Release Systems,” p. 14, 2011.

[62] M. N. SHETTY, *DISLOCATIONS AND MECHANICAL BEHAVIOUR OF MATERIALS*. PHI Learning Pvt. Ltd, 2013.

[63] A. K. Mishra, A. Roldan, and N. H. De Leeuw, “CuO Surfaces and CO2Activation: A Dispersion-Corrected DFT+U Study,” *J. Phys. Chem. C*, vol. 120, no. 4, pp. 2198–2214, 2016.

[64] V. Boiko, N. Vlasova, and A. Zaitsev, “Evaluation of the surface tension of tungsten carbides WC and WC-W 2 C by the results of the laser diffraction analysis of their milling with iron powder,” *Russ. J. Non-Ferrous Met.*, vol. 54, no. 6, pp. 493–496, 2013.

[65] A. Ghorai, A. Midya, R. Maiti, and S. K. Ray, “Exfoliation of WS_2 in the semiconducting phase using a group of lithium halides: a new method of Li intercalation,” *Dalt. Trans.*, vol. 45, no. 38, pp. 14979–14987, 2016.

[66] M. Ratoi, V. B. Niste, and J. Zekonyte, “WS2 nanoparticles – potential replacement for ZDDP and friction modifier additives,” *RSC Adv.*, vol. 4, no. 41, p. 21238, 2014.

[67] V. M. Rodriguez-Devecchis, L. Carbognani Ortega, C. E. Scott, and P. Pereira-Almao, “Use of Nanoparticle Tracking Analysis for Particle Size Determination of Dispersed Catalyst in Bitumen and Heavy Oil Fractions,” *Ind. Eng. Chem. Res.*, vol. 54, no. 40, pp. 9877–9886, 2015.

[68] R. R. Sahoo and S. K. Biswas, “Deformation and friction of MoS2 particles in liquid suspensions used to lubricate sliding contact,” *Thin Solid Films*, vol. 518, no. 21, pp. 5995–6005, 2010.

[69] G. N. Smith and J. Eastoe, “Controlling colloid charge in nonpolar liquids with surfactants,” *Phys. Chem. Chem. Phys.*, vol. 15, no. 2, pp. 424–439, 2013.

[70] H. Wu *et al.*, “Lubrication effectiveness investigation on the friendly capped MoS_2 nanoparticles,” *Lubr. Sci.*, vol. 29, no. 2, pp. 115–129, 2017.

[71] S. Roy and S. Sundararajan, “The effect of heat treatment routes on the retained austenite and Tribomechanical properties of carburized AISI 8620 steel,” *Surf. Coatings Technol.*, vol. 308, pp. 236–243, 2016.

[72] S. Hao, B. . Klamecki, and S. Ramalingam, “Friction measurement apparatus for sheet metal forming,” *Wear*, vol. 224, no. 1, pp. 1–7, 1999.

[73] X. Chen, R. A. Boulos, P. K. Eggers, and C. L. Raston, “Stabilization of 2D materials in water,” *Chem. Commun.*, pp. 0–9, 2012.

[74] Z. Chen, X. Liu, Y. Liu, S. Gunsel, and J. Luo, “Ultrathin MoS2 Nanosheets with Superior Extreme Pressure Property as Boundary Lubricants,” *Sci. Rep.*, vol. 5, no. 1, p. 12869, 2015.

[75] I. Lahouij, B. Vacher, J. M. Martin, and F. Dassenoy, “IF-MoS 2 based lubricants: Influence of size, shape and crystal structure,” *Wear*, vol. 296, pp. 558–567, 2012.

[76] F. Abate, V. D’Agostino, R. Di Giuda, and A. Senatore, “Tribological behaviour of MoS2 and inorganic fullerene-like WS2 nanoparticles under boundary and mixed lubrication regimes,” *Tribol. Surfaces Interfaces*, vol. 4, no. 2, pp. 91–98, 2010.

[77] L. Cizaire *et al.*, “Mechanisms of ultra-low friction by hollow inorganic fullerene-like MoS2 nanoparticles,” *Surf. Coatings Technol.*, vol. 160, no. 2–3, pp. 282–287, 2002.

[78] L. Yadgarov, V. Petrone, R. Rosentsveig, Y. Feldman, R. Tenne, and A. Senatore, "Tribological studies of rhenium doped fullerene-like MoS2 nanoparticles in boundary, mixed and elasto-hydrodynamic lubrication conditions," *Wear*, vol. 297, no. 1–2, pp. 1103–1110, 2013.

[79] V. An, Y. Irtegov, and C. De Izarra, "Study of tribological properties of nanolamellar WS 2 and MoS 2 as additives to lubricants," vol. 2014, no. 1971, 2014.

[80] A. Verma, W. Jiang, H. H. Abu Safe, W. D. Brown, and A. P. Malshe, "Tribological behavior of deagglomerated active inorganic nanoparticles for advanced lubrication," *Tribol. Trans.*, vol. 51, no. 5, pp. 673–678, 2008.

[81] "Characterization of Equilibrium Particle Size and Concentration in Oil-Based Nanolubricants A Thesis Submitted to the Faculty of the Graduate School of in partial fulfillment of the requirements for the degree of Master of Engineering Department of Mechan," no. December, 2012.

[82] R. Bari *et al.*, "Liquid phase exfoliation and crumpling of inorganic nanosheets," *Phys. Chem. Chem. Phys.*, vol. 17, no. 14, pp. 9383–9393, 2015.

[83] "The Application and Use of Soltex Products in Hydrocarbon Lubricants and Lubrication Systems – Base-Stocks," pp. 1–58.

[84] L. Guardia, J. I. Paredes, R. Rozada, S. Villar-Rodil, A. Martínez-Alonso, and J. M. D. Tascón, "Production of aqueous dispersions of inorganic graphene analogues by exfoliation and stabilization with non-ionic surfactants," *RSC Adv.*, vol. 4, no. 27, pp. 14115–14127, 2014.

[85] A. Moshkovith, V. Perfiliev, I. Lapsker, N. Fleischer, R. Tenne, and L. Rapoport, "Friction of fullerene-like WS2 nanoparticles: Effect of agglomeration," *Tribol. Lett.*, vol. 24, no. 3, pp. 225–228, 2006.

[86] P. U. Aldana, F. Dassenoy, B. Vacher, T. Le Mogne, and B. Thiebaut, "WS2 nanoparticles anti-wear and friction reducing properties on rough surfaces in the presence of ZDDP additive," *Tribol. Int.*, vol. 102, pp. 213–221, 2016.

[87] A. Moshkovith *et al.*, "Sedimentation of IF-WS2 aggregates and a reproducibility of the tribological data," *Tribol. Int.*, vol. 40, no. 1, pp. 117–124, 2007.

[88] X. Zhang *et al.*, "Synthesis of Ultrathin WS2 Nanosheets and Their Tribological Properties as Lubricant Additives," *Nanoscale Res. Lett.*, vol. 11, no. 1, p. 442, 2016.

[89] V. Bogdan, "WS 2 Nanoparticles -Potential Replacement for ZDDP and Friction Modifier Additives."

[90] D. Raichman, D. A. Strawser, and J. P. Lellouche, "Covalent functionalization/polycarboxylation of tungsten disulfide inorganic nanotubes (INTs-WS2)," *Nano Res.*, vol. 8, no. 5, pp. 1454–1463, 2014.

[91] D. Haba, T. Griesser, U. Müller, and A. J. Brunner, “Comparative investigation of different silane surface functionalizations of fullerene-like WS<inf>2</inf>,” *J. Mater. Sci.*, vol. 50, no. 15, pp. 5125–5135, 2015.

[92] G. Liu and N. Komatsu, “Readily Available ‘Stock Solid’ of MoS 2 and WS 2 Nanosheets through Solid-Phase Exfoliation for Highly Concentrated Dispersions in Water,” *ChemNanoMat*, vol. 2, no. 6, pp. 500–503, 2016.

[93] M. Gulzar *et al.*, “AW / EP behavior of WS 2 nanoparticles added to vegetable oil - based lubricant,” no. November, pp. 194–195, 2015.

[94] R. Kamatchi and S. Venkatachalapathy, “Parametric study of pool boiling heat transfer with nanofluids for the enhancement of critical heat flux: A review,” *Int. J. Therm. Sci.*, vol. 87, pp. 228–240, 2015.

[95] K. M. Koczkur, S. Mourdikoudis, L. Polavarapu, and S. E. Skrabalak, “Polyvinylpyrrolidone (PVP) in nanoparticle synthesis,” *Dalt. Trans.*, vol. 44, no. 41, pp. 17883–17905, 2015.

[96] A. Yella *et al.*, “Synthesis, characterization, and hierarchical organization of tungsten oxide nanorods: Spreading driven by Marangoni flow,” *J. Am. Chem. Soc.*, vol. 131, no. 48, pp. 17566–17575, 2009.

[97] M. Kole and T. K. Dey, “Role of interfacial layer and clustering on the effective thermal conductivity of CuO-gear oil nanofluids,” *Exp. Therm. Fluid Sci.*, vol. 35, no. 7, pp. 1490–1495, 2011.

[98] Y. Jazaa and S. Sundararajan, “Influence of surfactants on the tribological behavior of nanoparticle additives under boundary lubrication conditions.” Submitted to Tribology International.

[99] J. Zhang, Q. Wang, L. Wang, X. Li, and W. Huang, “Layer-controllable WS 2 - reduced graphene oxide hybrid nanosheets with high electrocatalytic activity for hydrogen evolution,” *Nanoscale*, vol. 7, no. 23, pp. 10391–10397, 2015.

[100] R. Bari *et al.*, “Liquid phase exfoliation and crumpling of inorganic nanosheets,” *Physi*, vol. 17, no. c, pp. 1–20, 2015.

[101] V. Srinivas, R. N. Thakur, A. K. Jain, and M. Saratchandra Babu, “Tribological Studies of Transmission Oil Dispersed With Molybdenum Disulfide and Tungsten Disulfide Nanoparticles,” *J. Tribol.*, vol. 139, no. 4, p. 041301, 2017.

[102] J. Sonali, N. Sandhyarani, and V. Sajith, “Tribological properties and stabilization study of surfactant modified MoS 2 nanoparticle in 15W40 engine oil,” vol. 1, no. 3, pp. 1–5, 2014.

[103] D. Maharaj and B. Bhushan, “Nanomechanical behavior of MoS2 and WS2 multi-walled nanotubes and carbon nanohorns,” *Sci. Rep.*, vol. 5, pp. 1–9, 2014.

[104] S. M. Hsu, “Nano-lubrication: Concept and design,” *Tribol. Int.*, vol. 37, no. 7, pp. 537–545, 2004.

[105] K. G. Binu, B. S. Shenoy, D. S. Rao, and R. Pai, “A Variable Viscosity Approach for the Evaluation of Load Carrying Capacity of Oil Lubricated Journal Bearing with TiO2 Nanoparticles as Lubricant Additives,” *Procedia Mater. Sci.*, vol. 6, no. Icmpc, pp. 1051–1067, 2014.

[106] A. Mariano, M. J. Pastoriza-Gallego, L. Lugo, A. Camacho, S. Canzonieri, and M. M. Piñeiro, “Thermal conductivity, rheological behaviour and density of non-Newtonian ethylene glycol-based SnO2nanofluids,” *Fluid Phase Equilib.*, vol. 337, pp. 119–124, 2013.

[107] J. C. Yang, F. C. Li, W. W. Zhou, Y. R. He, and B. C. Jiang, “Experimental investigation on the thermal conductivity and shear viscosity of viscoelastic-fluid-based nanofluids,” *Int. J. Heat Mass Transf.*, vol. 55, no. 11–12, pp. 3160–3166, 2012.

[108] J. Taha-Tijerina *et al.*, “Multifunctional nanofluids with 2D nanosheets for thermal and tribological management,” *Wear*, vol. 302, no. 1–2, pp. 1241–1248, 2013.

[109] S. Roy and A. Ghosh, “High Speed Turning of AISI 4140 Steel Using Nanofluid through Twin Jet SQL Syatem,” no. May, pp. 1–6, 2016.

[110] S. Roy and A. Ghosh, “High-speed turning of AISI 4140 steel by multi-layered TiN top-coated insert with minimum quantity lubrication technology and assessment of near tool-tip temperature using infrared thermography,” *Proc. Inst. Mech. Eng. Part B J. Eng. Manuf.*, vol. 228, no. 9, pp. 1058–1067, 2014.

[111] Y. Y. Wu, W. C. Tsui, and T. C. Liu, “Experimental analysis of tribological properties of lubricating oils with nanoparticle additives,” *Wear*, vol. 262, no. 7–8, pp. 819–825, 2007.

[112] V. An, Y. Irtegov, E. Anisimov, V. Druzyanova, N. Burtsev, and M. Khaskelberg, “Tribological properties of nanolamellar tungsten disulfide doped with zinc oxide nanoparticles,” *Springerplus*, vol. 4, no. 1, p. 673, 2015.

[113] H. Sade, A. Moshkovich, J.-P. Lellouche, and L. Rapoport, “Testing of WS2 Nanoparticles Functionalized by a Humin-Like Shell as Lubricant Additives,” *Lubricants*, vol. 6, no. 1, p. 3, 2018.

[114] Y. D. Zhang, J. S. Yan, L. G. Yu, and P. Y. Zhang, “Effect of nano-Cu lubrication additive on the contact fatigue behavior of steel,” *Tribol. Lett.*, vol. 37, no. 2, pp. 203–207, 2010.

[115] S. Soltanahmadi, A. Morina, M. C. P. van Eijk, I. Nedelcu, and A. Neville, “Tribochemical study of micropitting in tribocorrosive lubricated contacts: The influence of water and relative humidity,” *Tribol. Int.*, vol. 107, pp. 184–198, 2017.

[116] A. Greco, S. Sheng, J. Keller, and A. Erdemir, “Material wear and fatigue in wind turbine Systems,” *Wear*, vol. 302, no. 1–2, pp. 1583–1591, 2013.

[117] I. S. Al-Tubi, H. Long, J. Zhang, and B. Shaw, “Experimental and analytical study of gear micropitting initiation and propagation under varying loading conditions,” *Wear*, vol. 328–329, pp. 8–16, 2015.

[118] A. V. Olver, L. K. Tiew, S. Medina, and J. W. Choo, “Direct observations of a micropit in an elastohydrodynamic contact,” *Wear*, vol. 256, no. 1–2, pp. 168–175, 2004.

[119] B. Mahmoudi, “Investigation the effect of tribological coatings: WC/a-C:H and black oxide on micropitting behavior of SAE52100 bearing steel,” 2015.

[120] H. Singh, G. Ramirez, O. Eryilmaz, A. Greco, G. Doll, and A. Erdemir, “Fatigue resistant carbon coatings for rolling/sliding contacts,” *Tribol. Int.*, vol. 98, no. February, pp. 172–178, 2016.